JOPAT 24(2) 2407 – 2439, July – Dec. 2025 Edition.
ISSN2636 – 5448 https://dx.doi.org/10.4314/jopat.v24i2.13

Identification of Phytochemicals Inhibiting *Pf*CDPK-1, *Pf*CDPK-2, *Pf*CDPK-4, LDH and Hexokinase of *Plasmodium falciparum*

Moyosoluwa Precious Oyewole[1*], Taiwo Ooreoluwa Ojo[2], Akingbolagbo Daniel Ogunlakin[1]

Godwin Ayebaitari Berena[1], Oluyomi Stephen Adeyemi[1*]

[1] Medicinal Biochemistry and Toxicology Laboratory, Department of Biochemistry, Bowen University, Iwo 232101, Osun State, Nigeria. oyewoleprecious98@gmail.com; gowin.berena@bowen.edu.ng; yomibowa@yahoo.com

[2] Division of Computer-aided drug design, CompChem Hub, Oyo State, Nigeria. ojotawio718@gmail.com

ABSTRACT

Malaria remains a major global health challenge, exacerbated by the emergence of drug-resistant *Plasmodium falciparum* strains. To address this, novel therapeutic strategies targeting essential parasite proteins are urgently needed. In this study, we employed a computational drug discovery approach to identify potential inhibitors against five key *P. falciparum* proteins: cyclin-dependent kinases (*Pf*CDK1, *Pf*CDK2, *Pf*CDK4), hexokinase, and lactate dehydrogenase (*Pf*LDH). These proteins play critical roles in parasite cell cycle regulation and energy metabolism, making them attractive targets for selective inhibition. Phytochemicals were sourced from the LOTUS database—a curated repository of natural products derived from plants. Ligands were initially screened using Lipinski's Rule of Five (Ro5), drug-likeness criteria, and toxicity filters including mutagenicity, tumorigenicity, and irritability. Non-toxic candidates were subjected to molecular docking to evaluate binding affinities and interaction patterns with the target proteins. Molecular mechanics simulations were subsequently employed to assess the structural stability and energy profiles of the protein-ligand complexes. In addition, in silico ADMET profiling was performed to evaluate pharmacokinetic properties and safety parameters. Several compounds exhibited strong binding affinities and favorable interaction energies, particularly against *Pf*CDK4 and *Pf*LDH. Our findings show that the integration of natural product databases with computational screening and mechanics-based modeling proved effective in identifying promising antimalarial candidates, warranting further experimental validation.

Keywords: Drug discovery; Natural products; Molecular docking; Molecular mechanics

***Correspondence:** oyewoleprecious98@gmail.com; **yomibowa@yahoo.com**

INTRODUCTION

Malaria, caused by protozoan parasites of the genus *Plasmodium*, with *P. falciparum* being one of the devastating infectious diseases, remains a formidable global health challenge, particularly in sub-Saharan Africa, Southeast Asia, and parts of South America [1,2]. This disease is transmitted via the bite of infected female *Anopheles* mosquitoes accounting for approximately 247 million cases and 619,000 deaths globally in 2024, with children under five constituting the majority of fatalities. Despite the availability of antimalarial therapies [3], the emergence of drug-resistant strains has significantly undermined treatment efficacy, prompting the urgent need for novel therapeutic agents with distinct mechanisms of action [4].

The parasite's complex life cycle and its ability to rapidly develop resistance to antimalarial drugs underscore the urgent need for novel therapeutic strategies [5,6]. Targeting essential proteins in the parasite's life cycle offers a promising strategy for drug discovery [7]. Cyclin-dependent kinases (*Pf*CDK1, *Pf*CDK2, *Pf*CDK4) are pivotal regulators of cell cycle progression and schizogony in *P. falciparum* [8,9,10]. These kinases are structurally divergent from their human counterparts, making them attractive targets for selective inhibition. *Pf*CDK4, in particular, has been implicated in transmission-blocking mechanisms, highlighting its relevance for interrupting parasite propagation. In addition to regulatory kinases, metabolic enzymes such as hexokinase and lactate dehydrogenase (*Pf*LDH) are indispensable for parasite survival. *Pf* hexokinase catalyzes the phosphorylation of glucose to glucose-6-phosphate, initiating glycolysis—a pathway heavily relied upon by the parasite during its intraerythrocytic stages [11]. Structural studies have revealed *Plasmodium*-specific insertions in *Pf* hexokinase that influence ATP binding and tetrameric interface communication, offering unique sites for therapeutic intervention [12]. Additionally, *Pf*LDH, which converts pyruvate to lactate, is essential for anaerobic ATP production and exhibits significant structural divergence from human LDH, enabling selective targeting [13].

Natural products have long served as a rich source of bioactive compounds with antimalarial potential [14,15]. The LOTUS database (Linked Open natural products Universal Structure) is a curated, open-access repository of plant-derived compounds, offering detailed structural and taxonomic annotations [16]. In this study, we mined LOTUS to identify phytochemicals with potential anti plasmodial activity [17,18]. Preliminarily, selected compounds were screened for mutagenicity and toxicity using in silico ADMET profiling to ensure safety and drug-likeness. Subsequently, molecular docking was employed to evaluate the binding affinities and interaction profiles of non-toxic candidates with the five target proteins. Molecular mechanics simulations were used to assess the energy profiles and structural stability of the protein-ligand complexes, providing insights into conformational compatibility and potential inhibitory effects.

By integrating natural product screening with computational modeling, this study identifies safe and potent inhibitors of key *P. falciparum* proteins. The findings contribute to the growing body of evidence supporting plant-derived compounds as viable candidates in the fight against malaria and underscore the value of combining bioinformatics resources with structure-based drug design.

MATERIALS AND METHODS

Protein preparation *(PfCDPK-1, PfCDPK-2, PfCDPK-4, LDH and Hexokinase)*

The structures of *Pf*CDPK-2 (PDB ID: 4MVF; resolution: 2.0 Å; R-free: 0.230), *Pf*CDPK-4 (PDB ID: 4QOX; resolution: 2.75 Å; R-free: 0.266), LDH (PDB ID: 1T2C; resolution: 2.01 Å; R-free: 0.184), and hexokinase (PDB ID: 7ZZI; resolution: 2.80 Å; R-free: 0.268) were retrieved in biological assembly format from the RCSB Protein Data Bank (https://www.rcsb.org). Since a crystal structure for *Pf*CDPK-1(Average pLDDT = 86.69 High) was not available in the RCSB database, it was obtained from the AlphaFold protein structure database (AF-P62343-F1*)*. The biological assembly format of the proteins used for the molecular docking analysis are in their monomeric form. The protein structure was refined using PROPKA at pH 7.0 to predict pKa values and optimize the structure. The structure was then prepared for docking by filling in missing side chains, adding hydrogen atoms, and setting zero bond orders to metals. A minimization process was performed using the OPLS4 force field, converging every atom to an RMSD of 0.3 Å. Crystallographic water molecules were removed, except for those within 5.00 Å of the active site, as these waters may play a crucial role in mediating interactions between the protein and substrate. The resulting minimized protein structure was then used for molecular docking predictions.

Ligand generation and screening

Ligands were retrieved from the LOTUS database and screened using Lipinski rule of 5 (R05), drug likeness, mutagenicity,

tumorigenicity, and irritability. DataWarrior assesses "druglikeness" by checking for several properties, including Lipinski's rules (Molecular Weight, cLogP, H-bond donors, H-bond acceptors), and other metrics like polar surface area (PSA), rotatable bonds, and toxicity alerts (mutagenicity, tumorigenicity). The "druglikeness score" is calculated from these parameters to help validate a compound's potential as a drug candidate. The threshold used by the software ranks the toxicity of the compounds as "High, medium or Low" and all five screening rules were strictly enforced.

Molecular docking

The screened 26,610 ligands were submitted to the ligand docking panel together with their respective standards (Schrödinger Release 2022-4: Glide, Schrödinger, LLC, New York, NY, 2022) of Mav13.4 against the five protein targets. The receptor site was defined to be the grid dimension generated from site mapping. We set the ligand to dock or score at ≤ 500 atoms and not to dock or score ligands ≥100 rotatable bonds. The virtual screening was done using standard precision (SP) method employing flexible ligand sampling method. The maximum number of top poses to return per ligand was set to 5. The ligands' performance after virtual screening were ranked according to their glide score [19]. From this screening, only best hit compounds were chosen each for the protein targets identified to have the best interaction and binding affinity score. The best three compounds that outperformed the standard/control ligand used was selected in the study.

Post docking MM/GBSA binding free energy calculation

Methods based on molecular mechanics (such as MM/GBSA) are widely utilized techniques for approximating the binding free energy when small ligands interact with biological macromolecules [20]. The binding free energy (ΔG bind) was calculated using the Prime [21] MM/GBSA (Molecular Mechanics Generalized Born Surface Area) module within Maestro v13.4 (Schrödinger Release 2022-4: Prime, Schrödinger, LLC, New York, NY, 2022). Following the docking process, the selected compounds with the best binding affinity values, underwent a minimized sampling procedure using the OPLS4 force field. This procedure incorporated the Variable Dielectric Surface Generalized-Born (VSG) solvation model for polar solvation and the Solvent Accessible Surface Area (SASA) for non-polar solvation. The initial partial charges on the ligands (in their best poses) were retained, and van der Waals interactions were analyzed.

ADME and Toxicity evaluation

iDrug Web server, accessible at https://drug.ai.tencent.com/en [22] and PROTOX II was used to assess the phytochemical's pharmacokinetics features, including absorption, distribution, metabolism, excretion, and toxicity of the chosen compounds to help choose the optimal therapeutic candidate of the target proteins. The threshold used by The software ranks the toxicity of the compounds as "High, medium or Low", All five screening rules were strictly enforced.

RESULTS

Ligands screening

276,518 ligands were retrieved from the LOTUS database. After screening using the Lipinski rule of 5 (R05), drug likeness, mutagenicity, tumorigenicity, and irritability, the ligands were pruned down to 26,610 ligands as shown in supplementary table 1.

Structure-Activity Relationship (SAR) of Anti-Malarial Compounds

As shown in Figure 1, compounds 7383, 7384, and 8255 share a core indole ring system (a six-membered benzene ring fused to a five-membered nitrogen-containing pyrrole ring) with similar arrangement of other rings and a nitrogen atom at the top of the structure. The key differences are in the substituents on the rings as Compound 7384 has a methyl group (−CH3) attached that is absent in the others, Compound 8255 has a hydroxyl group (−OH) on its core scaffold, which is not present in 7383 or 7384. Compound 18620 and 18621 are very closely

related, differing only in the position of a single bond and the stereochemistry of a hydroxyl group. They both share a four-ring, polycyclic aromatic skeleton with arrangement of the carbon atoms and the attached hydroxyl (−OH) groups is almost identical. The most notable difference is the orientation of the hydroxyl group on one of the rings, which is indicated by the dashed line and the solid wedge.

Compound 21023 and 21024 molecules have the same complex cage-like structure with the same number of carbons, hydrogens, and oxygens and share an identical polycyclic framework with multiple ether bridges. The key difference lies in the stereochemistry of a hydroxyl group and a methyl group. The position and orientation of these groups relative to the rest of the molecule are different, which would lead to distinct three-dimensional shapes.

Compound 6395 and Compound 8286 have a central, fused three-ring system, both contain multiple hydroxyl (−OH) and ketone (=O) functional groups, which are key to their chemical reactivity and biological active. Compound 8286 has an additional ring attached to the core structure and a different arrangement of its hydroxyl groups, with one of them in a different position. The presence of the additional ring changes the overall size and shape of the molecule, which would significantly impact how it binds to a receptor or enzyme.

Compound 12876 and Compound 17603 contain a central, multi-ring system and have various functional groups attached. They have a shared characteristic of being complex, natural product-like molecules, often with a specific biological function.the most notable difference is their overall shape and the types of functional groups present. Compound 12876 has a fused, linear ring system with carboxylic acid groups (−COOH), while Compound 17603 has a more complex, branched and rigid polycyclic structure. Their different functionalities suggest they would interact with entirely different biological targets, despite both being complex organic molecules.

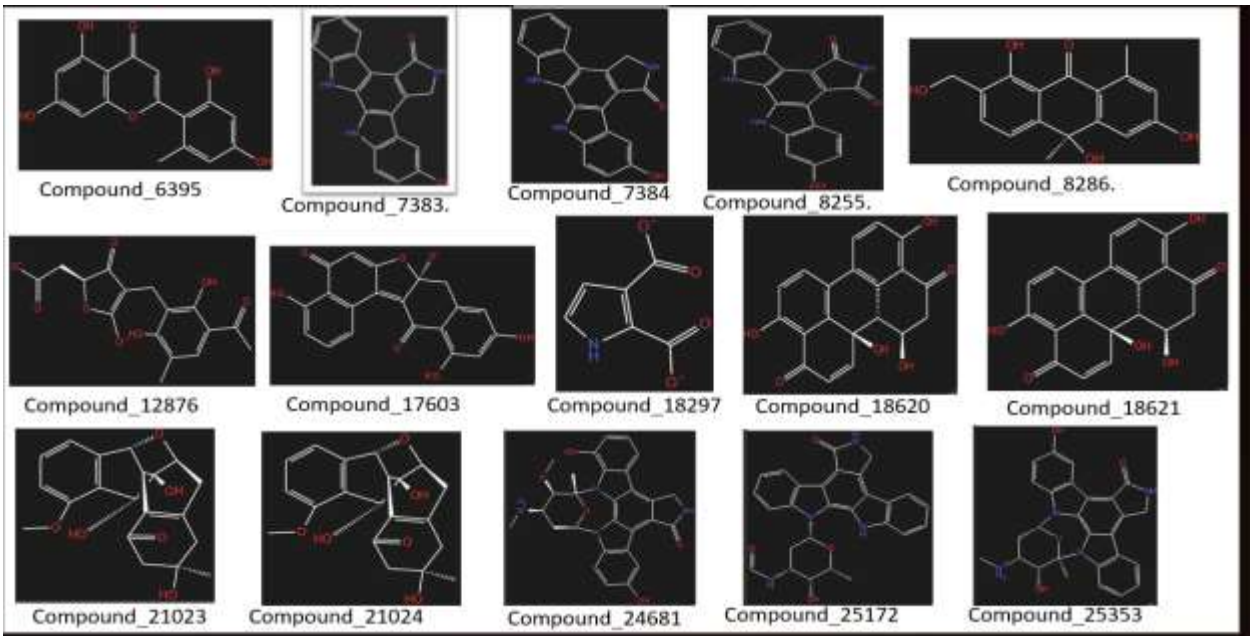

Figure 1;2D structure of anti-Malarial Compounds

Table 1; Compounds and their names

Compound ID	Name
Compound_6395.	11,25-dihydroxy-3-methoxy-2-methyl-4-(methylamino)-29-oxa-1,7,17-triazaoctacyclo[12.12.2.12,6.07,28.08,13.015,19.020,27.021,26]nonacosa-8(13),9,11,14,19,21(26),22,24,27-nonaen-16-one
Compound_7383.	3-methoxy-2-methyl-4-(methylamino)-29-oxa-1,7,17-triazaoctacyclo[12.12.2.12,6.07,28.08,13.015,19.020,27.021,26]nonacosa-8,10,12,14,19,21,23,25,27-nonaen-16-one
Compound_7384.	8-hydroxy-3-methoxy-2-methyl-4-(methylamino)-29-oxa-1,7,17-triazaoctacyclo[12.12.2.12,6.07,28.08,13.015,19.020,27.021,26]nonacosa-8,10,12,14,19,21,23,25,27-nonaen-16-one
Compound_8255.	5S,6R,7S,8R)-5,6,7,8-tetrahydroxy-2-(2-phenylethyl)-5,6,7,8-tetrahydrochromen-4-one
Compound_8286.	6R,7S)-6,7-dihydroxy-2-(2-phenylethyl)-5,6,7,8-tetrahydrochromen-4-one
Compound_12876.	6-hydroxy-3,13,23-triazahexacyclo[14.7.0.02,10.04,9.011,15.017,22]tricosa-1,4(9),5,7,10,15,17,19,21-nonaene-12,14-dione
Compound_17603.	2-(2,4-dihydroxy-6-methylphenyl)-5,7-dihydroxychromen-4-one
Compound_18297	3-[(2S,5S)-5-(2-methylpropyl)-3,6-dioxopiperazin-2-yl]propanoic acid
Compound_18620.	7,13,17-trihydroxy-12-oxapentacyclo[]henicosa-1,3(8),4,6,10,16(21),17,19-octaene-9,15-dione
Compound_18621.	4-(2,4-dihydroxy-3,5-dimethylphenyl)-4-oxobutanoic acid
Compound_21023.	12S,12aS,12bR)-4,9,12,12b-tetrahydroxy-2,11,12,12a-tetrahydro-1H-perylene-3,10-dione
Compound_21024.	(12S,12aS,12bR)-4,9,12,12b-tetrahydroxy-2,11,12,12a-tetrahydro-1H-perylene-3,10-dione
Compound_24681.	2-methyl-1H-pyrrole-3-carboxylic acid
Compound_25172.	5,11-dihydroxy-13-methoxy-5-methyl-19-oxapentacyclo[8.8.1.01,10.02,7.012,17]nonadeca-2(7),8,12(17),13,15-pentaene-3,18-dione
Compound_25353.	5,11-dihydroxy-13-methoxy-5-methyl-19-oxapentacyclo[8.8.1.01,10.02,7.012,17]nonadeca-2(7),8,12(17),13,15-pentaene-3,18-dione

Molecular docking

Binding profile of *plasmodium falciparum* CDPK-1 (calcium-dependent protein kinase 1)

Following the virtual screening process, three new top-performing compounds—25172, 24681, and 25353—showed superior interactions with the active site of *Pf*CDPK-1 when compared to the reference compound purfalcamine. Notably, all the three compounds formed two hydrogen bonds with the key residue Tyr148, suggesting its vital role in anchoring ligands within the protein pocket (Figures 3 – 5). In addition, Glu146 appeared consistently across all compounds as a significant hydrogen bonding partner. Glu152 also contributed as a stabilizing interaction, particularly present in Compounds 24681 and 25353 as both hydrogen and non-hydrogen bonding partners.

Conversely, the reference compound as shown figure 2 interacted with Arg60, Glu152, Asn196, and Asp212, yet only Asn196 and Asp212 reside

within the protein's active site—possibly explaining its relatively lower binding affinity. All selected compounds demonstrated higher binding affinities than the standard, with Compound 25172 exhibiting the strongest value at –10.030 kcal/mol.as shown in table 2.

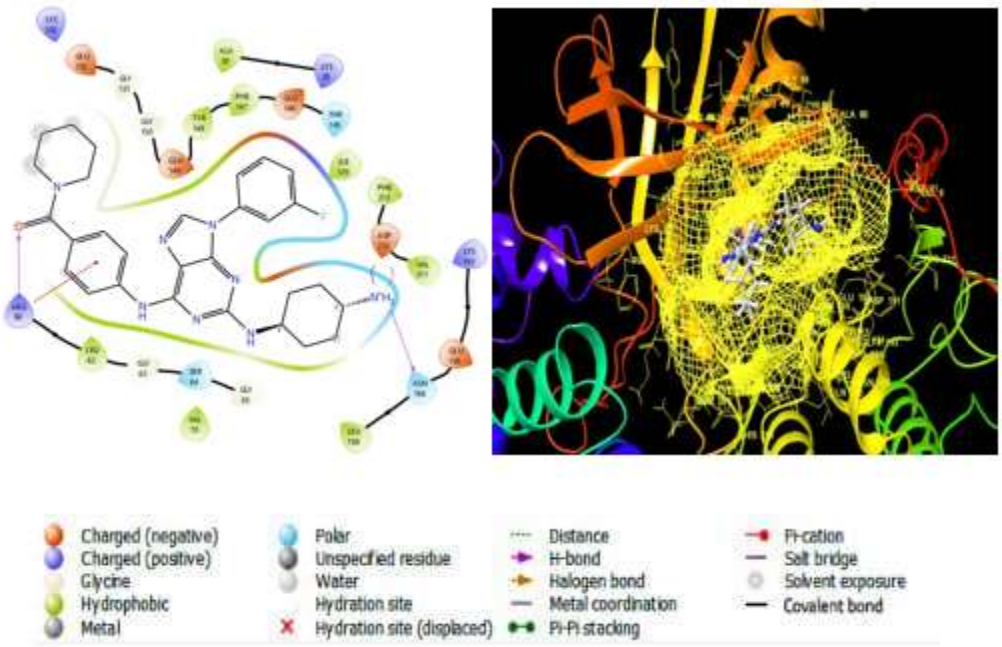

Figure 2: 2D and 3D interactions of *Plasmodium falciparum* CDPK-1(calcium-dependent protein kinase 1) and co-crystallized ligand (Purfalcamine)

Table 2: Binding profile of compounds to *Plasmodium falciparum* CDPK-1 (calcium-dependent protein kinase 1

S/N	Hydrogen bond	Other bonds	Binding affinity
Standard			
Purfalcamine	Arg60, Glu152, **Asn196, Asp212**	**Asp212**	-8.421
Selected compounds			
Compound 25172	Glu146, **Tyr148,** Glu193		-10.030
Compound 24681	Glu146, **Tyr148 (2),** Glu152	Glu152	-9.793
Compound 25353	Glu146, **Tyr148 (2),** Glu152	Glu152	-9.525

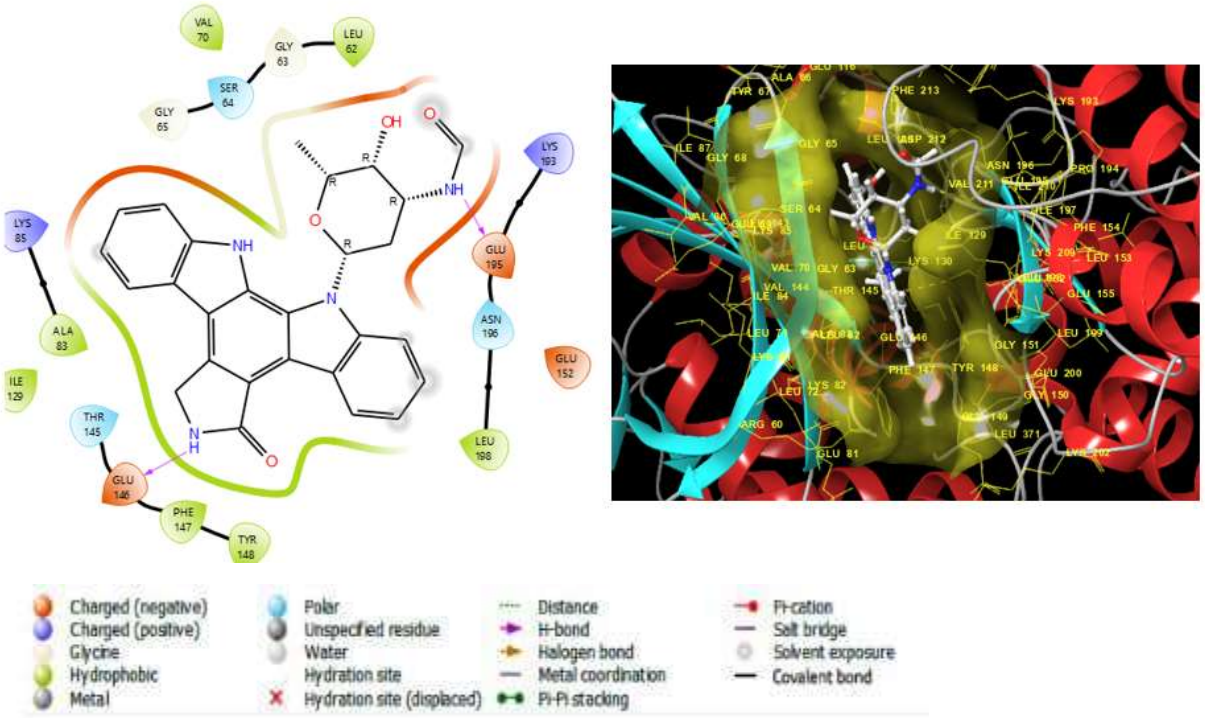

Figure 3: 2D and 3D interactions of *Plasmodium falciparum* CDPK-1(calcium-dependent protein kinase 1) and Compound 25172

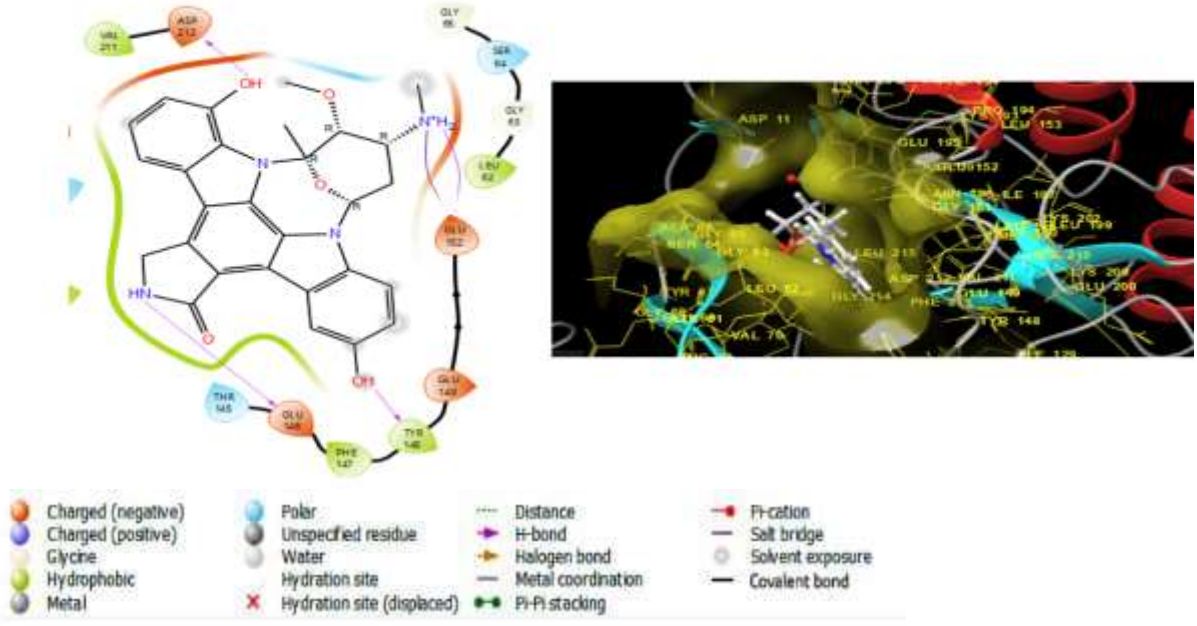

Figure 4: 2D and 3D interactions of *Plasmodium falciparum* CDPK-1(calcium-dependent protein kinase 1) and Compound 24681

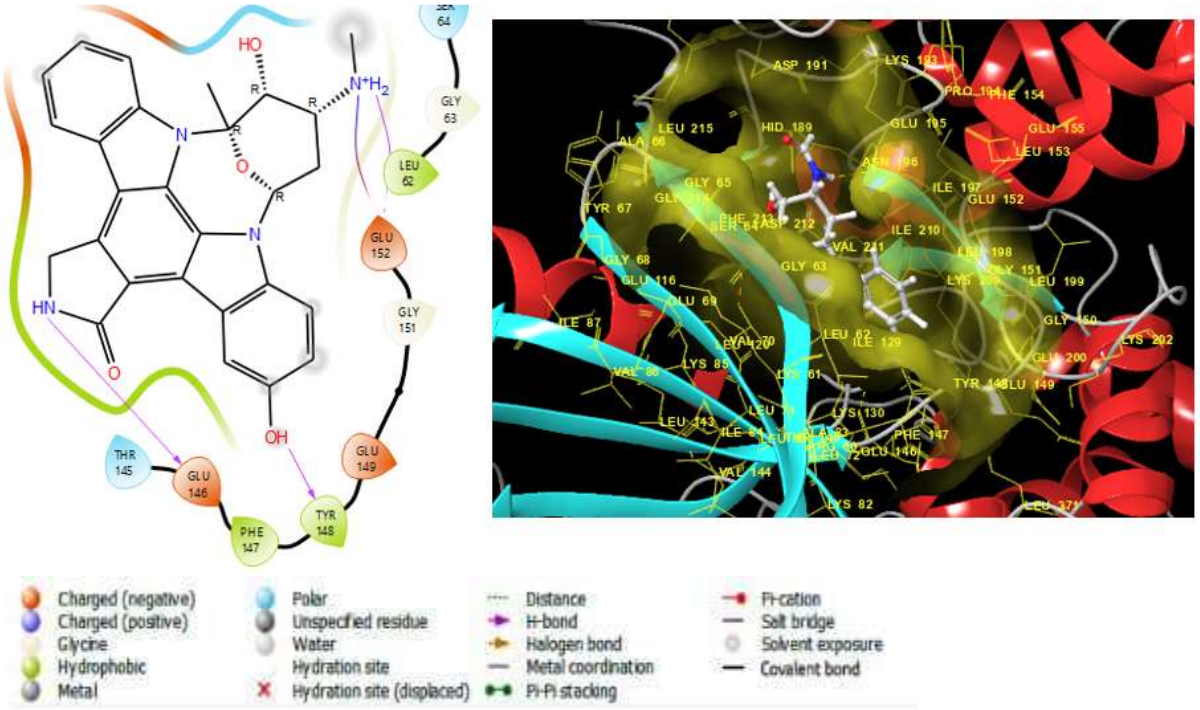

Figure 5: 2D and 3D interactions of *Plasmodium falciparum* CDPK-1(calcium-dependent protein kinase 1) and Compound 25353

Binding profile of *plasmodium falciparum* CDPK-2 (calcium-dependent protein kinase 2

Interaction of the compounds with *Pf*CDPK2 identified 3 compounds that are most likely to inhibit the activity of this protein when compared with the reference compound (staurosporine), which formed a single hydrogen bond with Cys149, alongside several hydrophobic and polar contacts involving Leu78, Gly79, Leu199, Glu196, Gly151, Ser150, Ala99, Val86, Ile212, and Lys101 (Figure 6). Despite its broad interaction profile, its binding affinity was relatively weak at –6.022 kcal/mol, likely due to limited hydrogen bonding in the core active region.

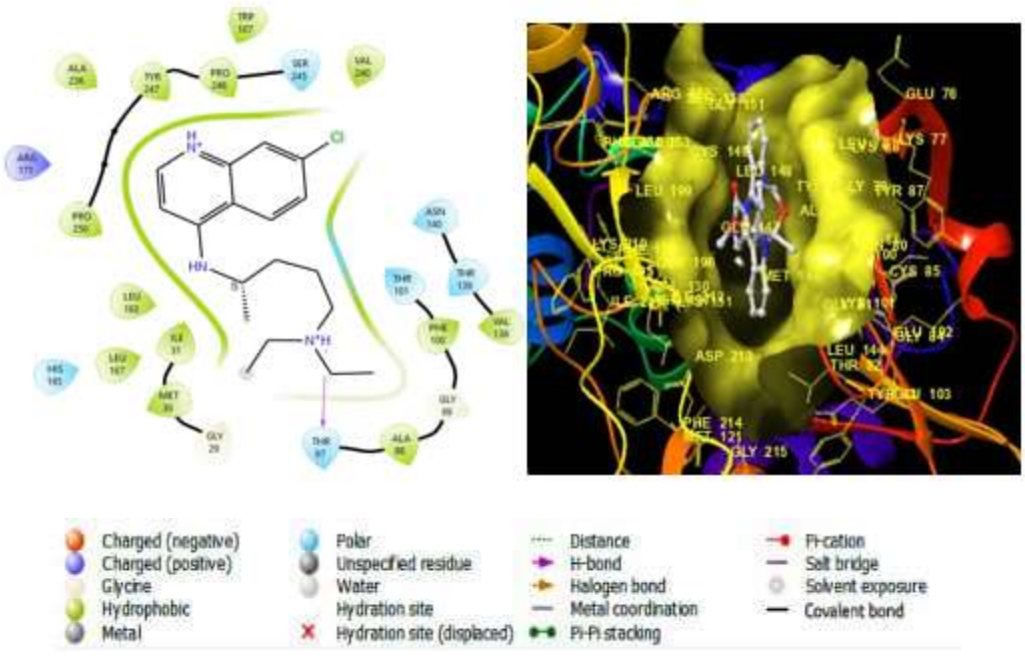

Figure 6: 2D and 3D interactions of *Plasmodium falciparum* CDPK-2(calcium-dependent protein kinase 2) and co-crystallized ligand (staurosporine)

In contrast, the three newly screened ligands—compounds 7383, 7384, and 8255—demonstrated significantly stronger binding affinities and more specific interactions with key residues of *Pf*CDPK-2 (Figures 7 – 9). Each compound formed hydrogen bonds with Cys149, reinforcing its role as a critical residue in ligand binding. Furthermore, recurring interactions with Glu147 in all three hits suggest it may also be central to effective binding. Notably, compound 7383 interacted with both Lys101 and Ile212, enhancing its contact surface within the active pocket and resulting in the highest binding affinity of –10.972 kcal/mol as shown in table 3.

Table 3; Binding profile of compounds to *Plasmodium falciparum* CDPK-2 (calcium-dependent protein kinase 2

S/N	Hydrogen bond	Other bonds	Binding affinity
Standard			
Staurosporin	**Cys149**	**Leu78, Gly79, Leu199, Glu196, Gly151, Ser150, Ala99, Val86, Ile212, Lys101**	-6.022
Selected compounds			

Compound 7383	Glu147, Cys149, **Lys101, Ile212**		-10.972
Compound 7384	Glu147, **Cys149 (2)**		-10.564
Compound 8255	Glu147, **Cys149**, Asp213		-10.554

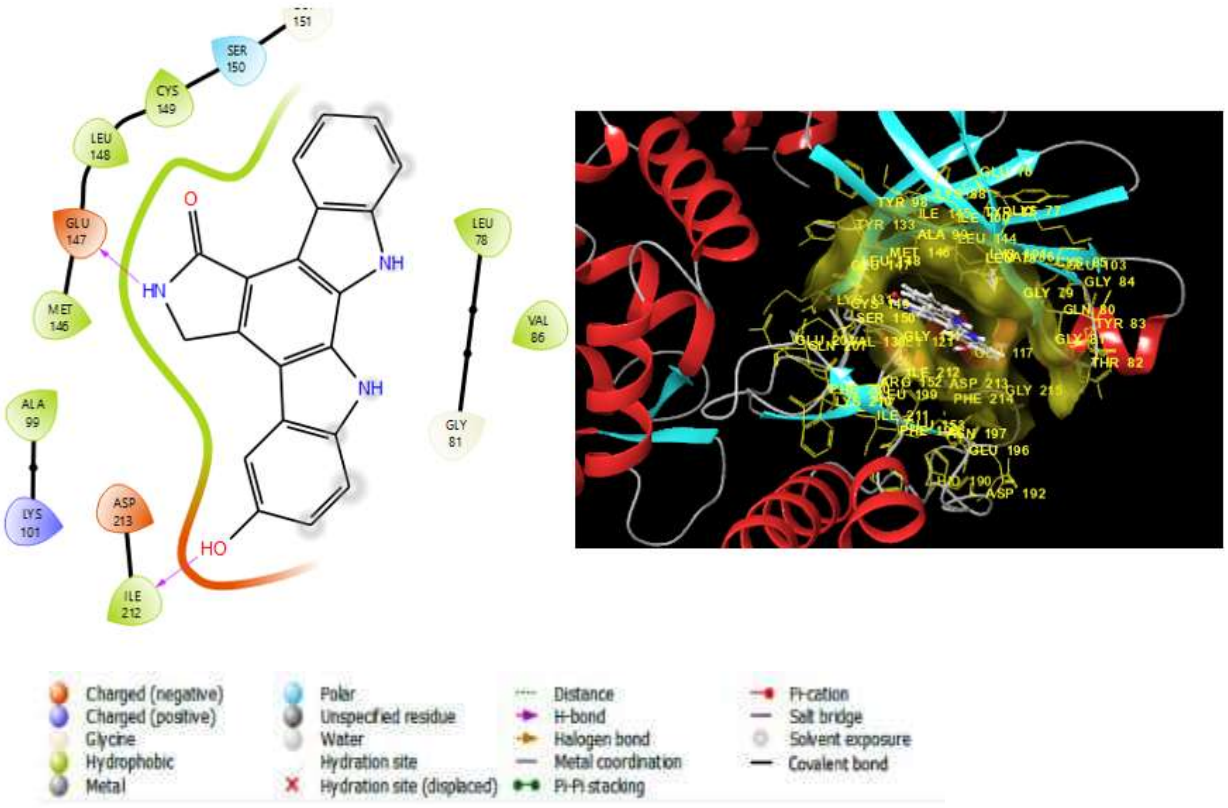

Figure 7: 2D and 3D interactions of *Plasmodium falciparum* CDPK-2(calcium-dependent protein kinase 2) and 7483

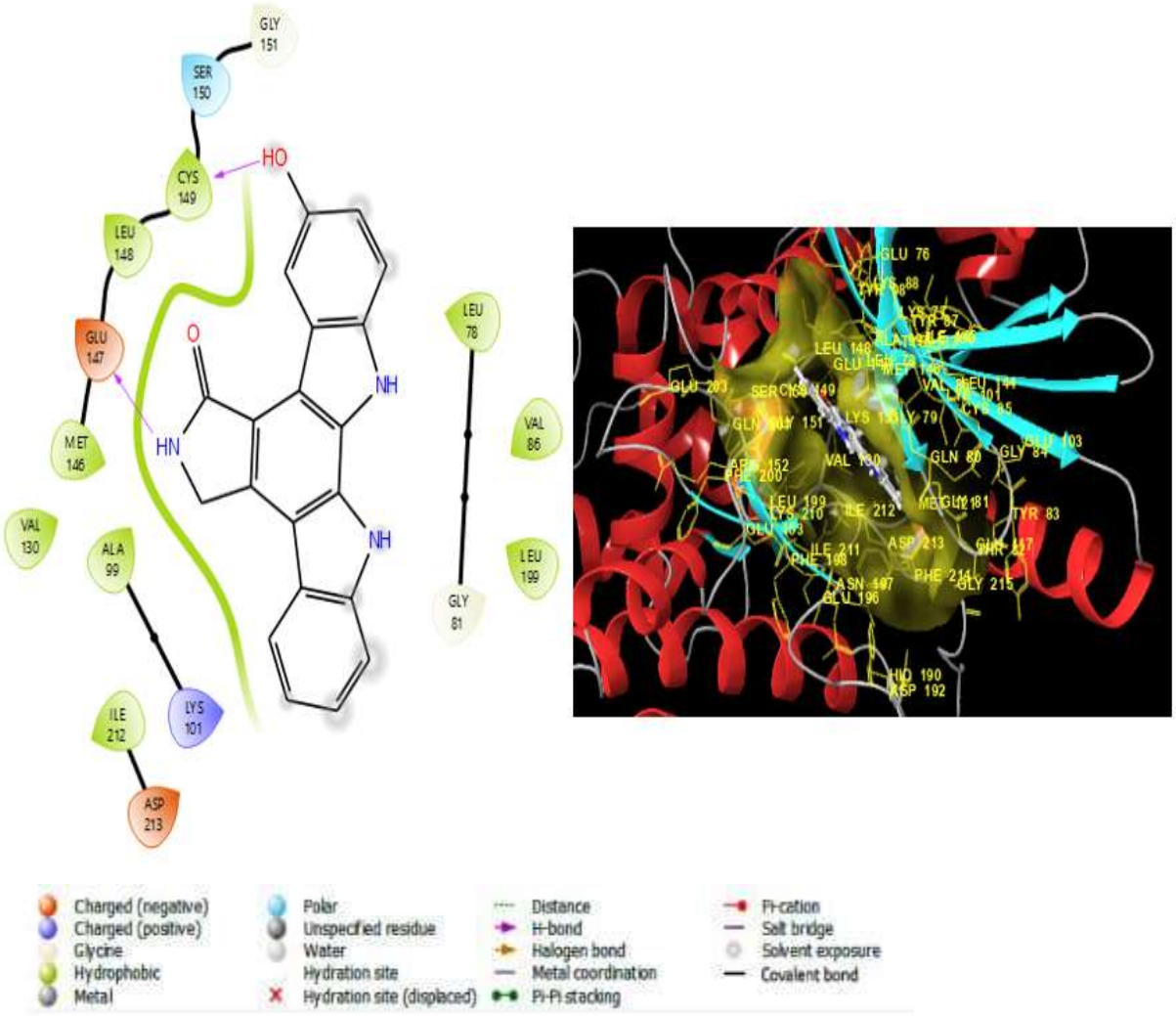

Figure 8: 2D and 3D interactions of *Plasmodium falciparum* CDPK-2(calcium-dependent protein kinase 2) and 7484

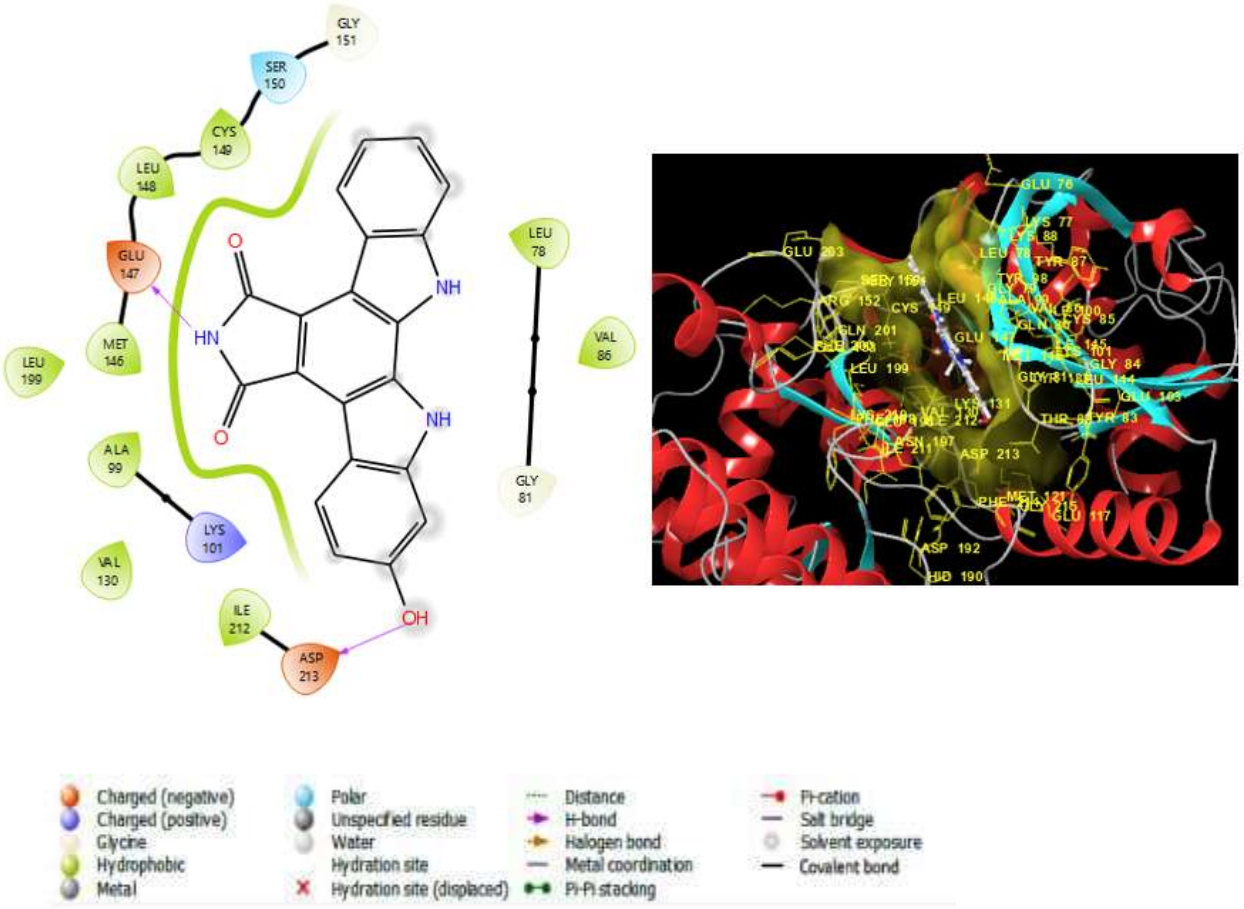

Figure 9: 2D and 3D interactions of *Plasmodium falciparum* CDPK-2(calcium-dependent protein kinase 2) and 8255

Binding profile of *plasmodium falciparum* CDPK-4 (calcium-dependent protein kinase 4)

Consequently, interaction of the compounds with *Pf*CDPK4 revealed that 17603, 8286, and 6395—demonstrated significantly improved binding profiles relative to the reference compound pyrazole 3,4-d pyrimidine (Figures 10 – 13). The standard formed hydrogen bonds with Gly74, Tyr150, and Glu154, alongside other polar and hydrophobic contacts with Glu154 and Glu197, resulting in a binding affinity of –5.131 kcal/mol, which is notably weaker than all selected hits.

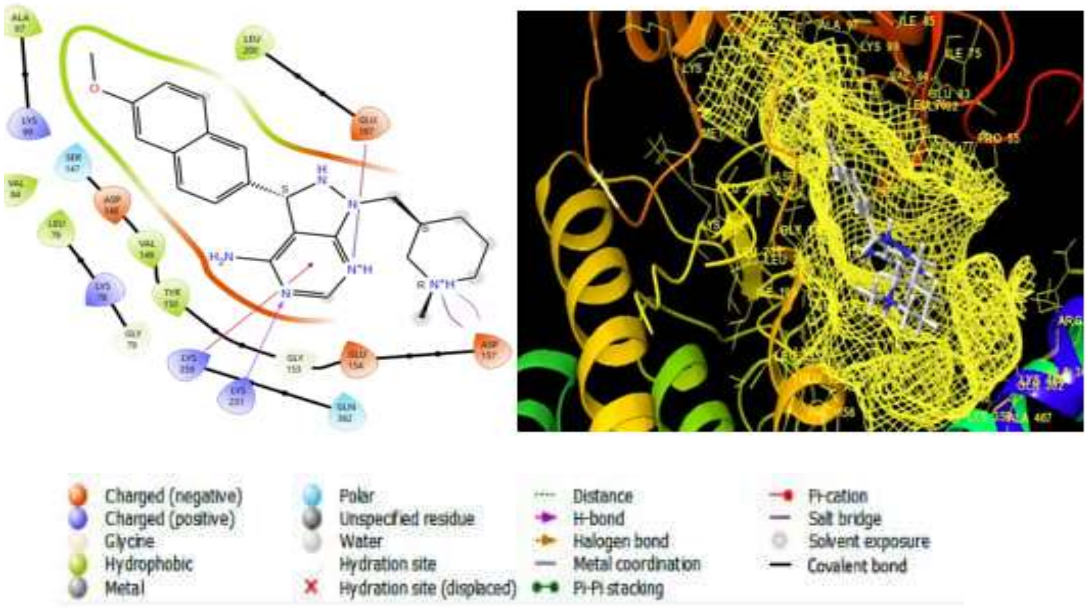

Figure 10: 2D and 3D interactions of *Plasmodium falciparum* CDPK-4 (calcium-dependent protein kinase 4) and co-crystallized ligand (pyrazole 3, 4-d pyrimidine)

All three lead compounds formed hydrogen bonds with Glu154, a residue that appears central to ligand stability in the protein's active site. Tyr150 and Asp148 also emerged as recurring hydrogen bonding partners, underscoring their importance across effective binders.

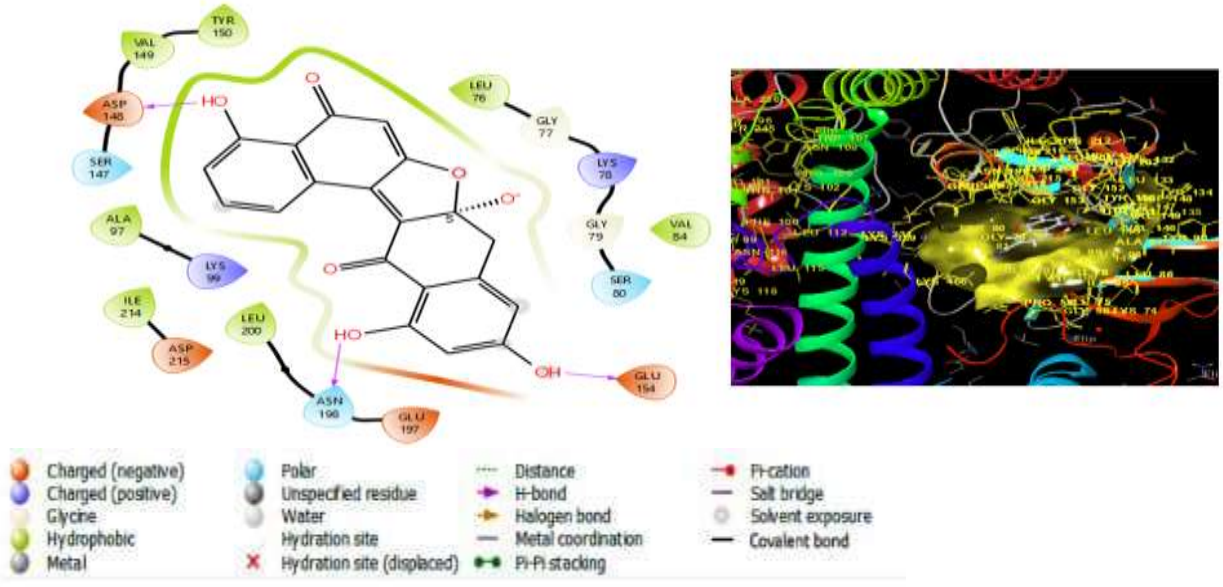

Figure 11: 2D and 3D interactions of *Plasmodium falciparum* CDPK-4 (calcium-dependent protein kinase 4) and Compound 17603

Compound 17603 as shown in figure 11 had the highest binding affinity (–9.935 kcal/mol), forming five hydrogen bonds including a double interaction with Tyr150 and additional contact with Asn198 and Lys99.Compound 8286 also engaged multiple hydrogen bonding residues—Glu154, Lys99, Tyr150, and Asp148—leading to a strong binding affinity of –9.428 kcal/mol.Compound 6395 was unique in sharing Glu154 and Glu197 interactions with the reference compound, but with improved hydrogen bonding to Tyr15 and Asp148, yielding a binding affinity of –9.410 kcal/moas shown in table 4.

Table 4; Binding profile of compounds to *Plasmodium falciparum* CDPK-4(calcium-dependent protein kinase 4

S/N	Hydrogen bond	Other bonds	Binding affinity
Standard			
Pyrazole 4-d pyrimidine	**GLys74, Tyr150, Glu154**	**Glu154, Glu197**	**-5.131**
Selected compounds			
Compound 17603	**Glu154, Asn198, Lys99, Tyr150(2), Asp148**		**-9.935**
Compound 8286	**Glu154, Lys99, Tyr150, Asp148**		**-9428**
Compound 6395	**Glu154, Glu197, Tyr15, Asp148**		**-9.410**

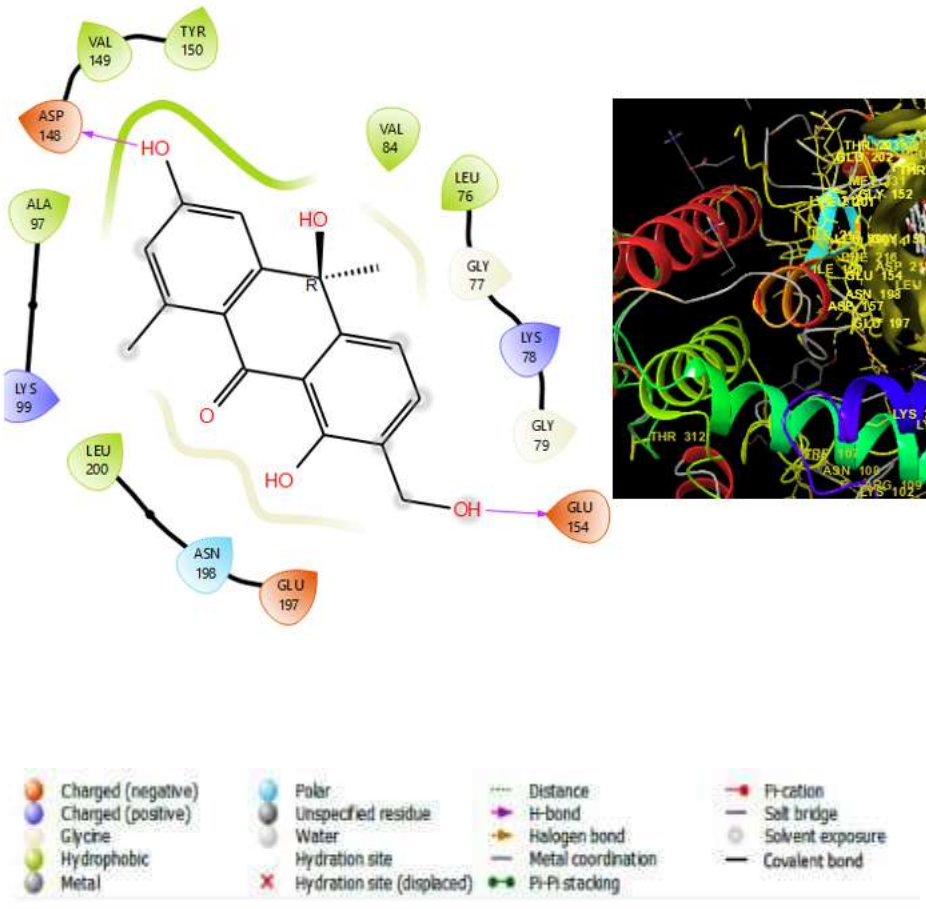

Figure 12: 2D and 3D interactions of *Plasmodium falciparum* CDPK-4 (calcium-dependent protein kinase 4) and Compound 8286

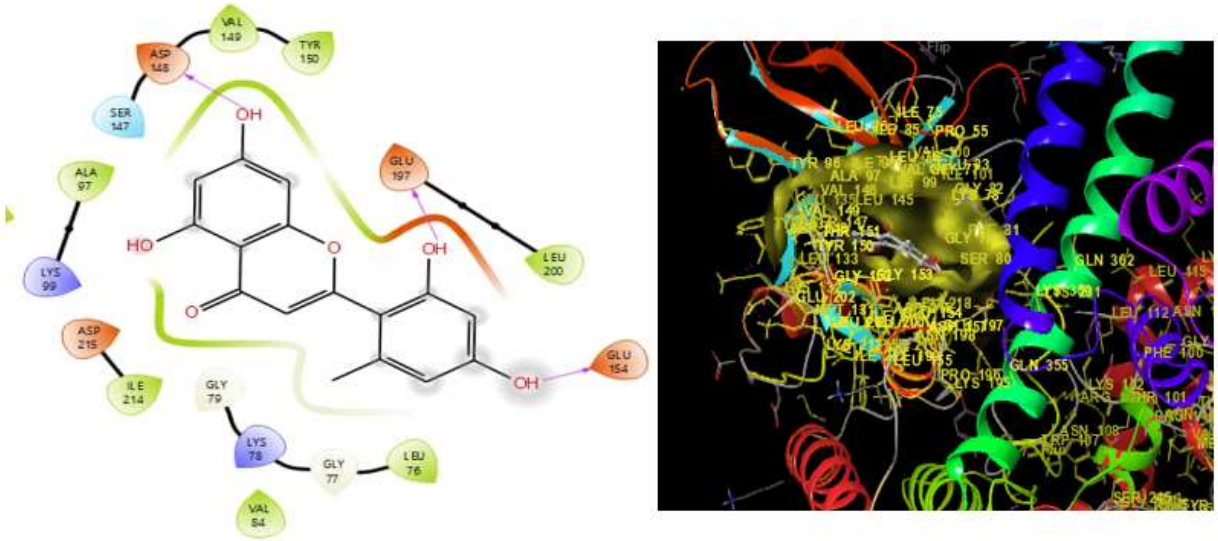

Figure 13: 2D and 3D interactions of *Plasmodium falciparum* CDPK-4 (calcium-dependent protein kinase 4) and Compound 6395

Binding profile of compounds to *Plasmodium falciparum* hexokinase (*PfHK*)

Furthermore, the standard reference compound ebselen showed hydrogen bonding interactions with Ser436 and Thr268, resulting in a relatively modest binding affinity of –4.003 kcal/mol(Figure14).

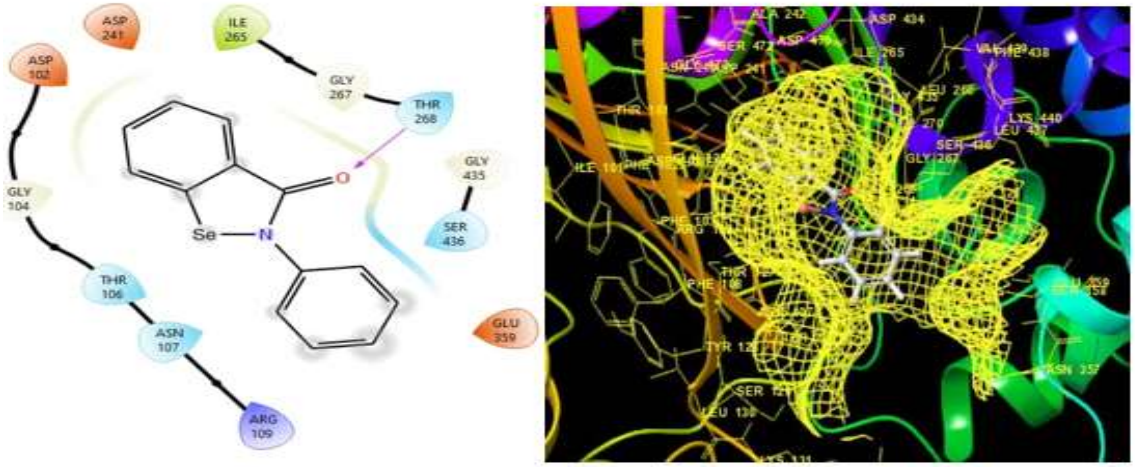

Figure 14: 2D and 3D interactions of *Plasmodium falciparum* hexokinase and co-crystallized ligand (Ebselen)

Three selected compounds—21023, 21024, and 18297—exhibited notably stronger binding interactions (Figures 15 – 17). Compounds 21023 and 21024 both formed hydrogen bonds with Glu359 and Ser358, leading to identical and significantly improved binding affinities of –7.423 kcal/mol. Compound 18297 demonstrated a unique hydrogen bonding network involving Thr268 (with two contacts), Ser436, and Asn107, achieving an affinity of –7.275 kcal/mol, also notably higher than the standard. as shown in table 5.

Table 5; Binding profile of compounds to *Plasmodium falciparum* hexokinase

S/N	Hydrogen bond	Other bonds	Binding affinity
Standard			
Ebselen	**Ser436, Thr268**		-4.003
Selected compounds			
Compound 21023	**Glu359, Ser358**		-7.423
Compound 21024	**Glu359, Ser358**		-7.423
Compound 18297	**Thr268(2),** Ser436, **Asn107**		-7.275

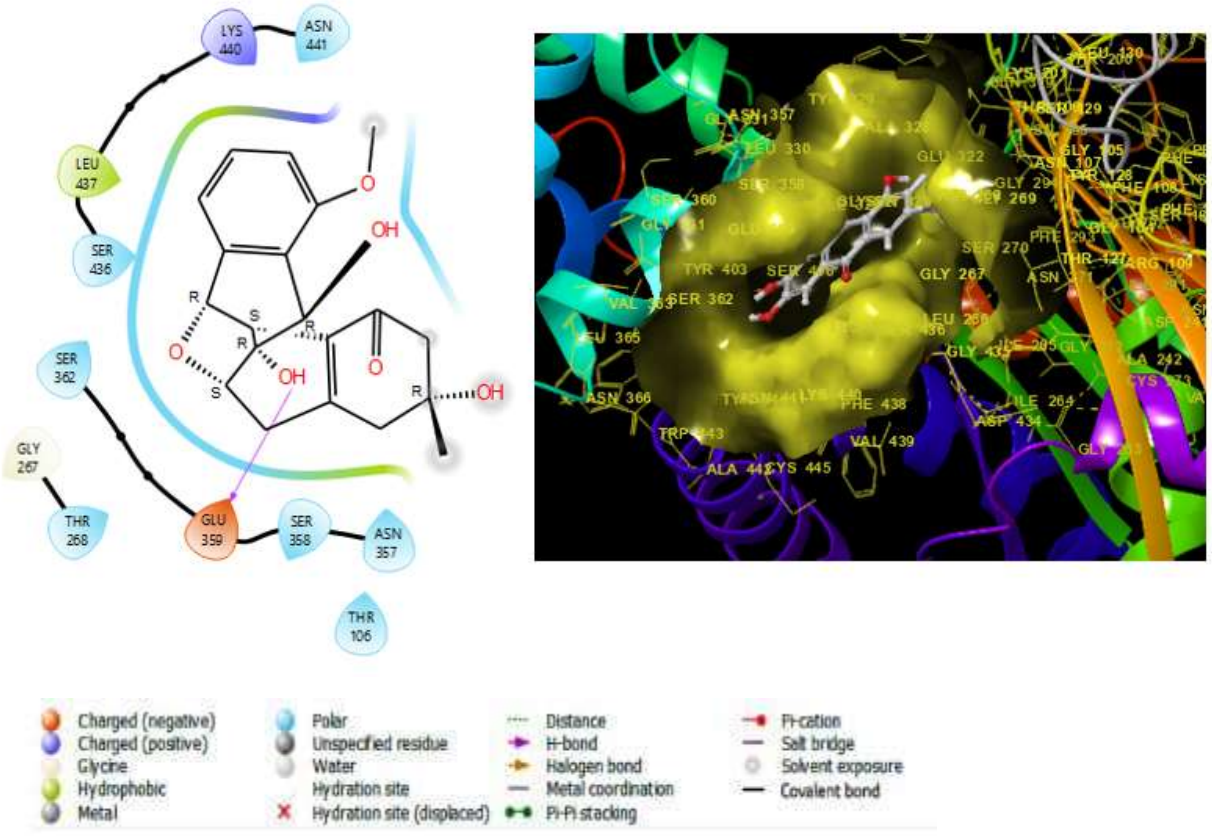

Figure 15: 2D and 3D interactions of *Plasmodium falciparum* hexokinase and Compound 21023

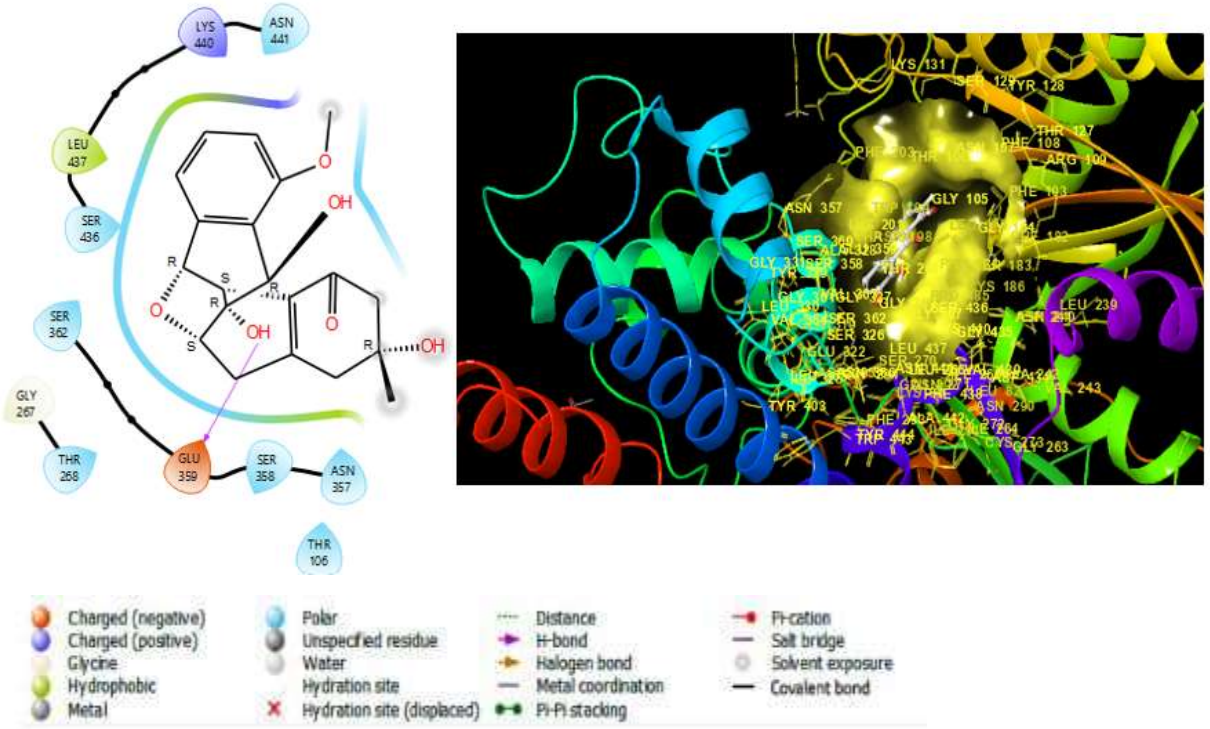

Figure 16: 2D and 3D interactions of *Plasmodium falciparum* hexokinase and Compound 21024

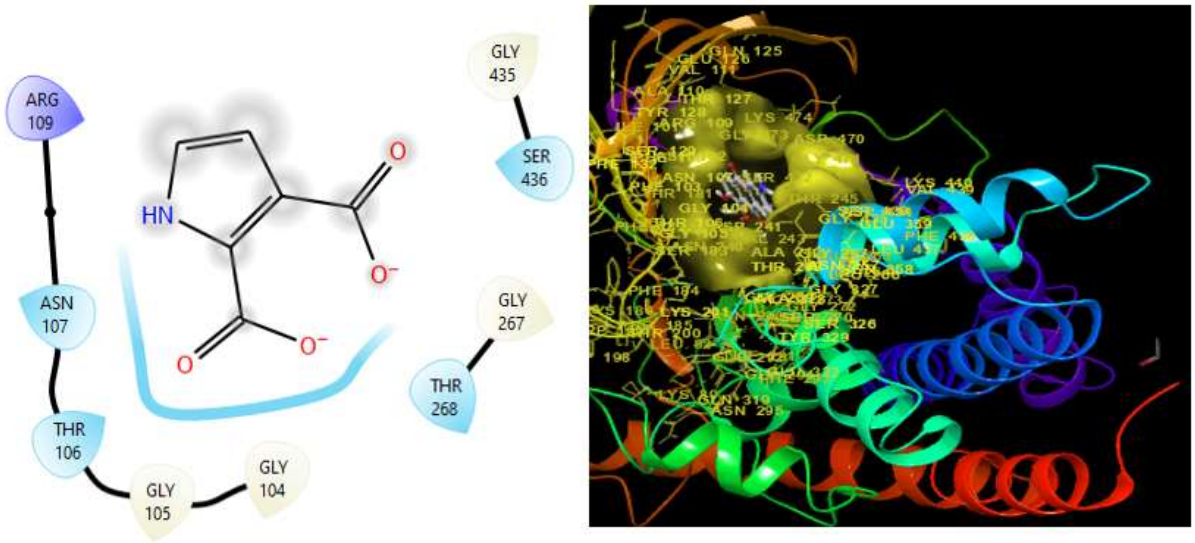

Figure 17: 2D and 3D interactions of *Plasmodium falciparum* hexokinase and Compound 18297

Binding profile of compounds to *Plasmodium falciparum* lactate dehydrogenase (*PfLDH*)

Finally, interaction recorded for LDH showed that chloroquine which is the reference standard formed hydrogen bonds with Thr97 and Arg171, resulting in a binding affinity of –4.673 kcal/mol, which is considerably lower than that of the selected ligands (Figure 18).

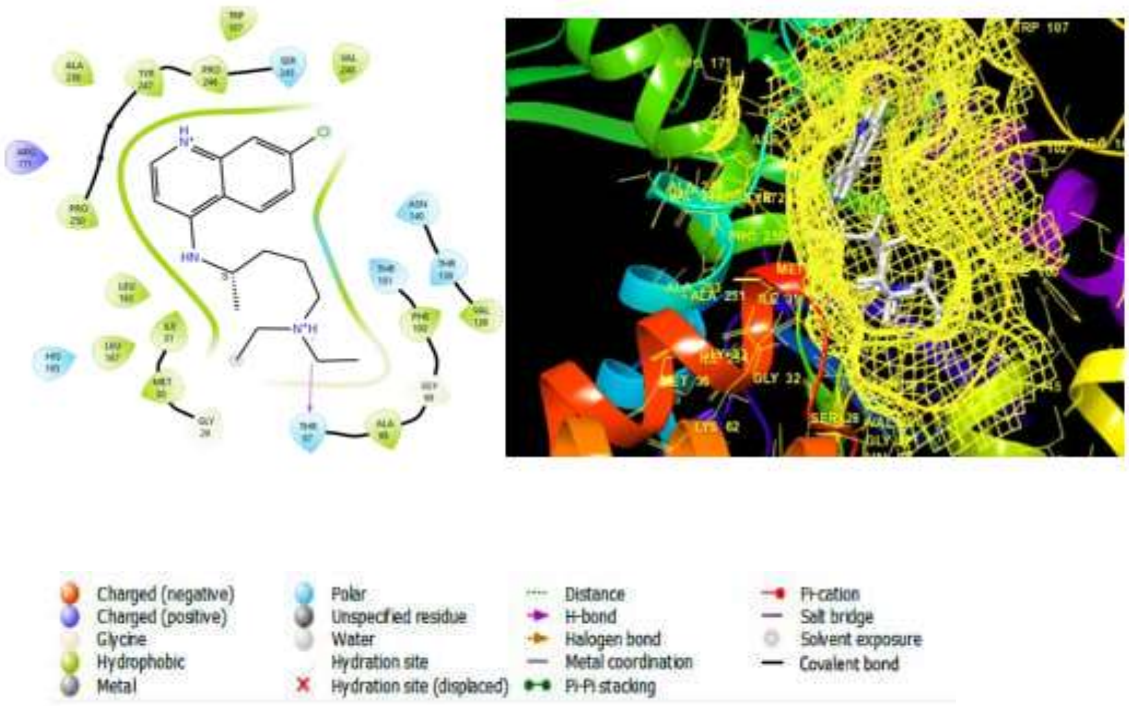

Figure 18: 2D and 3D interactions of *Plasmodium falciparum* lactase dehydrogenase and co-crystallized ligand (chloroquine)

Three compounds—12876, 18620, and 18621—demonstrated significantly stronger binding affinities (Figures 19 – 21), suggesting enhanced interaction with key residues within the protein's active site: Compound 12876 formed hydrogen bonds with Arg171, Ile31, and Thr101 and maintained additional bonding with Arg171, resulting in the highest binding affinity of –9.065 kcal/mo. Compound 18620 interacted through hydrogen bonds with His195, Thr97, Pro266, and Asn140, achieving an affinity of –8.437 kcal/mol. Compound 18621 formed similar interactions to 18620, including His195, Thr97, Thr101, and Asn140, yielding a slightly stronger binding affinity of –8.457 kcal as shown in table 6

Table 6; Binding profile of compounds to *Plasmodium falciparum* lactate dehygonesae

S/N	Hydrogen bond	Other bonds	Binding affinity
Standard			
Chloroquine	**Thr 97,** Arg171		-4.673
Selected compounds			
Compound 12876	Arg171, **Ile31**, **Thr101**	Arg171	-9.065
Compound 18620	His195, **Thr97**, Pro266, **Asn140**		-8.437
Compound 18621	His195, **Thr97**, **Thr101**, **Asn140**		-8.457

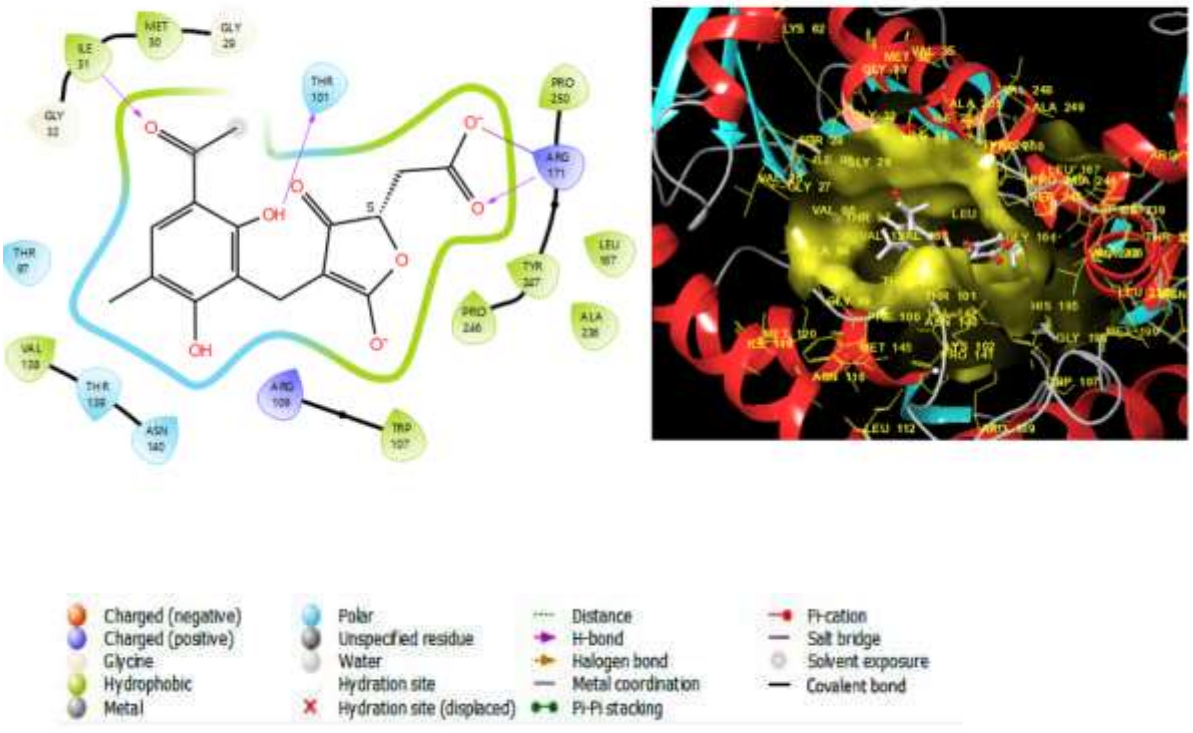

Figure 18: 2D and 3D interactions of *Plasmodium falciparum* lactate dehydrogenase and Compound 12876

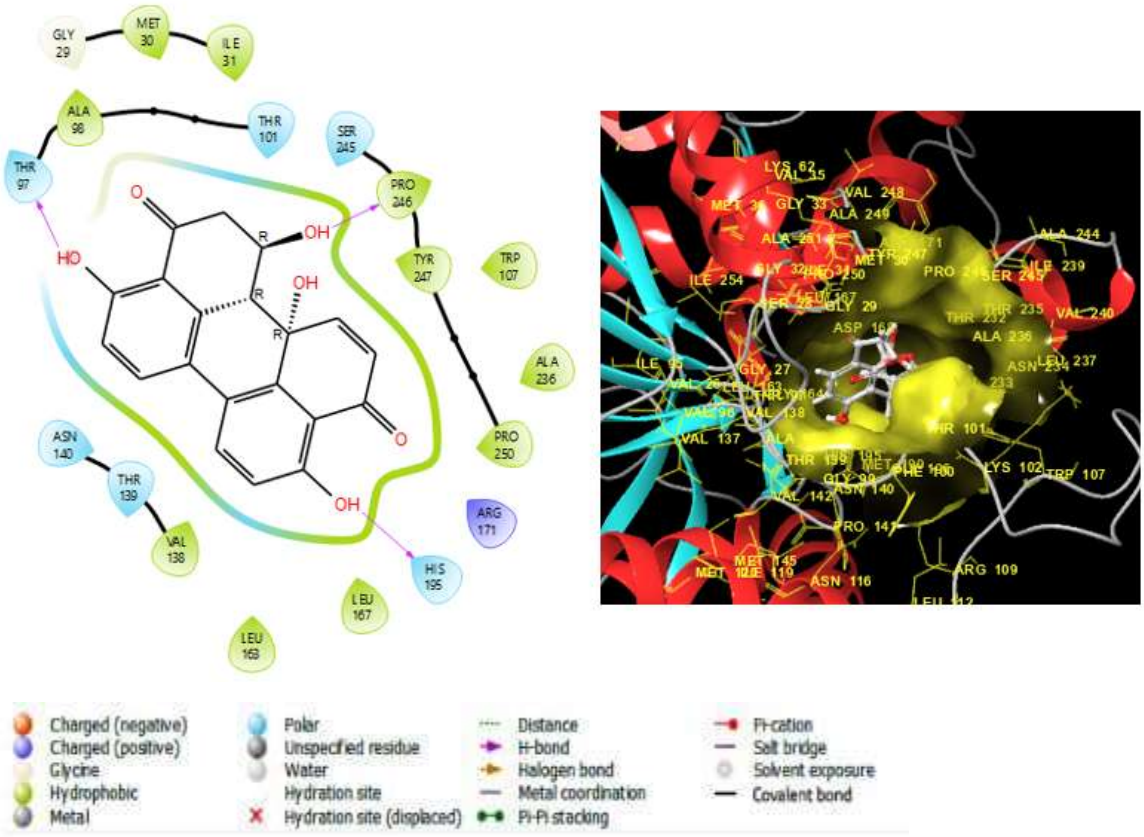

Figure 20: 2D and 3D interactions of *Plasmodium falciparum* lactate dehydrogenase and Compound 18620

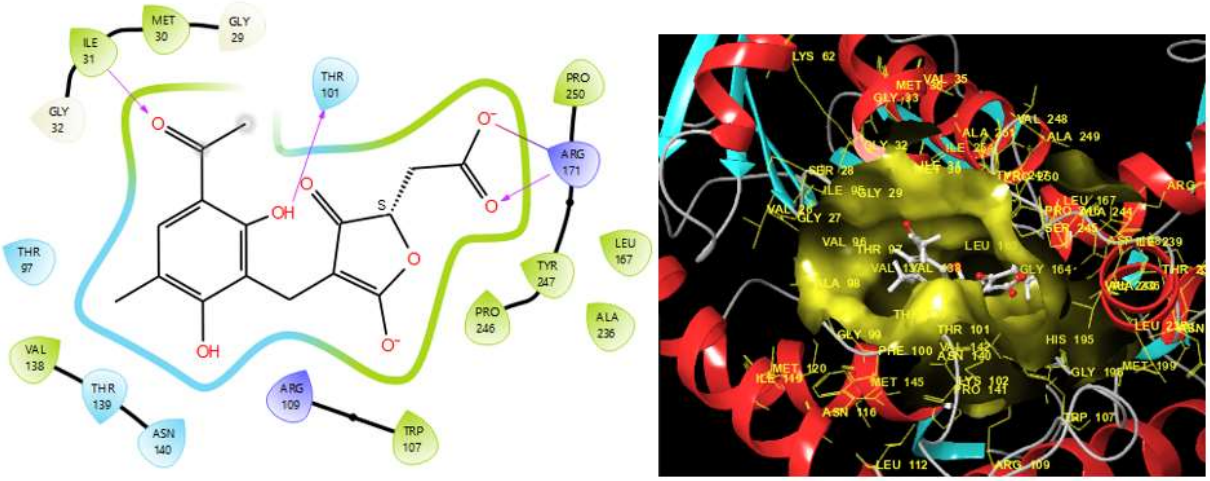

Figure 21: 2D and 3D interactions of *Plasmodium falciparum* lactate dehydrogenase and Compound 18621

Post docking *MM/GBSA* binding free energy calculation

Free energy binding is a measure of the energy change associated with the binding of two molecules, such as protein and a ligand. It depicts the thermodynamic property between the bound and unbound state of the molecules. Interestingly, as seen from the binding affinity result, the same trend of binding free energy was observed. As shown in Table 7, All compounds selected across the 5 protein targets out-performed the standard drugs. This energetically favourable interaction observed furthers validate the molecular docking selection process of the selected compounds.

Table 7: *GBSA binding free energy calculation*

Compound/Parameter	MM-GBSA$_{\Delta G_Bind}$ (kcal/ mol)	MM-GBSA$_{\Delta G_H\text{-}Bond}$ (kcal/ mol)	MM-GBSA$_{\Delta G_Bind_vdW}$	MM-GBSA$_{\Delta G_Bind_Solv}$
***Pf*CDPK1**				
Purfalcamine	-68.77	-1.92	-64.41	29.45
Compound_24681	-71.81	-4.15	-29.75	133.45
Compound_25172	-73.77	-4.23	19.53	84.30
Compound_25353	-71.62	-4.04	-31.57	76.42
***Pf*CDPK2**				
Staurosporin	-37.84	-3.06	-36.27	35.01
Compound_7383	-54.66	-7.10	-54.44	111.12
Compound_7384	-53.78	-5.33	-35.33	86.44
Compound_8255	-51.11	-5.54	49.00	93.33
***Pf*CDPK4**				
Pyrazole-3,4-d pyrimidine	-35.97	-1.13	-37.74	-11.32
Compound_6395	-49.45	-4.23	-45.55	23.3
Compound_8286	-50.33	-4.40	-54.44	-45.33
Compound_17603	-57.35	-5.69	-60.43	-34.58
LDH				
Chloroquine	-37.13	-0.63	-42.02	89.68
Compound_12876	-65.33	-6.45	-35.20	34.52
Compound_18620	-56.54	-5.55	-45.33	46.44
Compound_18621	-55.55	-4.88	-29.65	46.77
HEXOKINASE				
Ebselen	-16.39	-0.63	-24.73	31.68
Compound_18297	-37.21	-4.96	-24.55	33.45
Compound_21023	-40.33	-4.56	-33.54	33.59
Compound_21024	-35.65	-4.88	-41.22	-40.21

ADMET RESULT

The *in silico* ADMET evaluation (Table 8) provides crucial insights into the pharmacokinetic and safety profiles of the selected compounds. Caco-2 permeability, a measure of passive intestinal absorption, showed a wide range of values (1.03 to 17.04) across all candidates. Compounds with high permeability values (above 10) are predicted to be readily absorbed from the small intestine. However, many compounds with moderate permeability (Caco-2 = 2.59) still exhibited high Human Intestinal Absorption (HIA) values (0.91), suggesting that active transport mechanisms may contribute significantly to their uptake. Conversely, compounds with lower HIA scores (0.25) are likely to have poor intestinal absorption, rendering them unsuitable for oral administration.Oral bioavailability is the most critical metric for an orally administered drug, and it showed a significant range (18–65%). While some compounds displayed high bioavailability (above 58%), others with very low values (below 18%) are considered non-viable oral drug candidates, regardless of their HIA. This discrepancy highlights the critical impact of first-pass metabolism on systemic exposure.P-glycoprotein (P-gp) inhibition was also evaluated. A high P-gp inhibition score (0.84) is a double-edged sword: it may increase a drug's own bioavailability by preventing efflux from intestinal cells but also poses a significant risk of dangerous drug-drug interactions by causing co-administered drugs to accumulate to toxic levels. A low P-gp inhibition score (e.g., 0.01) is generally a desirable characteristic, as it minimizes interference with this critical efflux pump.A wide range of plasma protein binding (PPB) values (56% to 92%) was observed. High PPB (87% to 92%) could limit the free drug concentration available for therapeutic action, potentially necessitating higher doses to achieve efficacy.

Metabolic stability was assessed through predicted interactions with cytochrome P450 (CYP) enzymes. A key finding was the wide variation in predicted human clearance values. High positive scores (0.93) indicate efficient elimination, a desirable trait to prevent drug accumulation. Conversely, very low positive scores (0.06) suggest a slow elimination rate, which could lead to drug accumulation over time. The most concerning values were negative scores (-1.3, -1.18), which, in a computational context, are strong red flags suggesting poor or negligible elimination and a high risk of systemic accumulation and toxicity.

CYP induction is another critical parameter. High induction scores (0.64–0.94) indicate a strong potential to accelerate the metabolism of co-administered drugs, posing a significant risk of drug-drug interactions and reducing therapeutic efficacy. In contrast, low induction scores (0.09) are a favorable characteristic.A consistent and significant safety concern across all evaluated compounds was the potential for genotoxicity. All candidates demonstrated extremely high scores (0.78–1.00), suggesting a high probability of causing genetic damage. Other toxicity risks, such as mutagenicity and hERG inhibition, varied among compounds, providing a basis for selecting candidates with a more favorable overall safety profile. Some compounds showed very low hERG inhibition (0.01), suggesting a minimal risk of cardiotoxicity. The diverse toxicity profiles highlight the importance of evaluating multiple safety parameters to identify the most promising and least risky drug candidate.

Table 8: Pharmacokinetic properties of selected compounds

	Properties	**C_25172**	**C_24681**	**C_25353**	**C_7383**	**C_7384**	**C_8255**	**C_17603**	**C_8286**	**C_6395**	**C_21023**	**C_21024**	**C_18297**	**C_122876**	**C_18620**	**C_18621**
ABSORPTION	Caco2 Permeability	2.59	1.71	1.48	2.56	2.52	3.23	6.7	6.47	6.47	16.76	17.04	1.53	1.03	4.0	4.0
	P-gp Inhibition	0.84	0.94	0.93	0.05	0.05	0.1	0.17	0.01	0.01	0.85	0.03	0.01	0.01	0.02	0.02
	HIA	0.91	0.98	0.99	0.97	0.97	0.99	0.93	0.98	0.98	1	0.97	0.25	1	0.51	0.51
	Oral Bioavailabilty	28%	18%	19%	19%	9	2%	0%	7%	7%	8%	6%	5%	9%	8%	8%
DISTRIBUTION	Plasma Protein Binding (Human)	92%	92%	87%	88%	8%	9%	0%	7%	7%	8%	0%	6%	6%	2%	2%
	CYP Induction	0.17	0.09	0.1	0.68	0.68	0.66	0.85	0.78	0.78	0.31	0.64	0.26	0.32	0.94	0.94
METABOLISM	CYP1A2 Inhibition	0.47	0.51	0.48	0.93	0.93	0.93	0.94	0.83	0.83	0.28	0.04	0.09	0.14	0.48	0.48
	CYP2C19 Inhibition	0.27	0.25	0.23	0.05	0.05	0.04	0.58	0.34	0.34	0.33	0.07	0.09	0.02	0.29	0.29
	CYP2C9 Inhibition	0.27	0.32	0.26	0.08	0.08	0.07	0.74	0.52	0.52	0.29	0.01	0.02	0.02	0.26	0.26

	CYP2D6 Inhibition	0.38	0.34	0.38	0.28	0.27	0.08	0.39	0.32	0.32	0.17	0.01	.02	.04	.05	.05
	CYP3A4 Inhibition	0.44	0.56	0.44	0.62	0.63	0.45	0.11	0.19	0.19	0.29	0	0.02	0.02	0.2	0.2
	Human Clearance	0.06	1.3	1.18	0.35	0.35	0.93	0.99	1.11	1.11	0.15	0.07	0.88	0.37	0.98	0.98
EXCRETION	hERG Inhibition	0.31	0.14	0.18	0.01	0.01	0	0	0	0	0	0	0.01	0	0	0
TOXICITY	Ames Toxicity	0.42	0.6	0.62	0.74	0.74	0.93	0.81	0.89	0.89	0.09	0.09	0.05	0.23	0.82	0.82
	Hek293 Toxicity	0.75	0.69	0.63	0.25	0.25	0.21	0.37	0.06	0.06	0.12	0.11	0.01	0.03	0.1	0.1
	Hepatic Toxicity	0.5	0.73	0.75	0.75	0.74	0.74	0.62	0.5	0.5	0.66	0.66	0.47	0.89	0.56	0.56
	DILI	0.88	0.92	0.93	0.92	0.92	0.94	0.78	0.31	0.31	0.4	0.28	0.87	0.85	051	0.51
	Genotoxicity	0.99	1	1	0.99	0.99	0.99	0.97	0.89	0.89	0.85	0.78	0.88	0.91	0.92	0.92
	Carcinogenicity	0.26	0.02	0.19	0.32	0.32	0.28	0.43	0.39	0.39	0.39	0.27	0.24	0.27	0.24	0.24
	Mutagenicity	0.01	0.56	0.02	0.06	0.06	0.04	0.06	0.19	0.19	0.04	0.06	0.81	0.09	0.06	0.06

DISCUSSION

From an initial pool of 276,518 ligands retrieved from the LOTUS database, a refined set of 26,610 compounds was obtained through rigorous screening based on the Lipinski's Rule of Five (Ro5), drug-likeness, and toxicity filters including mutagenicity, tumorigenicity, and irritability. These criteria are essential for identifying compounds with favorable pharmacokinetic and safety profiles [23,24,25].

In silico screening of a diverse set of compounds against the malaria protein target yielded a number of promising inhibitors. A detailed structural analysis reveals clear structure-activity relationships (SARs) within this group, providing critical insights for future anti-malarial drug design [26]. The most potent inhibitory activities were observed in compounds sharing an indole ring system (Compounds 7383, 7384, and 8255). This conserved scaffold likely functions as a primary pharmacophore, providing the foundational structure for key interactions within the protein's active site. The variations within this series highlight the critical role of substituents in modulating binding affinity [27]. The addition of a methyl group on compound 7384 and a hydroxyl group on compound 8255 are calculated to influence binding energies, suggesting that these groups may participate in distinct intermolecular interactions, such as hydrophobic packing or hydrogen bonding, respectively, with specific amino acid residues of the protein. Beyond the indole series, other structural relationships emerged. Compounds 18620 and 18621 present a fascinating case of stereoisomeric analogs. While sharing an identical core carbon skeleton and functional groups, they differ only in the three-dimensional orientation of a single hydroxyl group. Our docking results suggest that this subtle difference in stereochemistry is sufficient to alter their fit within the binding pocket, likely leading to a different array of stabilizing interactions and thus varying inhibitory activities. This finding underscores the paramount importance of stereochemistry in drug-receptor binding, where the precise 3D shape of a molecule dictates its pharmacological effect. Compounds 6395 and 8286 represent another class of structural analogs. They share a complex, multi-ring fused system but differ in the number and arrangement of their rings and functional groups. The presence of additional rings in compound 8286 alters the overall shape and size of the molecule, which may explain its specific binding profile compared to compound 6395. Similarly, the different arrangements of hydroxyl and ketone groups suggest that they might interact with different parts of the binding site or with different amino acid residues, leading to distinct binding modes and potentially different mechanisms of inhibition. Compounds 12876, 17603, 21023, and 21024 demonstrate that effective inhibitors of the same protein can arise from completely different chemical scaffolds. While compounds 21023 and 21024 are stereoisomers, 12876 and 17603 have fundamentally different core structures. This suggests that the protein's active site may be flexible or contain multiple sub-pockets that can accommodate a wide range of chemical motifs. This finding is valuable as it broadens the scope of future compound libraries for screening, suggesting that novel inhibitors may not be restricted to scaffolds that resemble known anti-malarial drugs.

Molecular docking analysis successfully identified three novel compounds—25172, 24681, and 25353—as potent inhibitors of *Pf*CDPK-1, demonstrating superior binding affinities compared to the known inhibitor, purfalcamine. These findings provide valuable insights into the key molecular interactions necessary for inhibiting this crucial malaria protein. The superior binding of the three lead compounds is attributed to their specific interactions within the active site of *Pf*CDPK-1. All three compounds consistently formed hydrogen bonds with Tyr148 and Glu146. The conservation of these interactions across the three most active compounds suggests that Tyr148 and Glu146 are not merely involved in ligand binding but are critical for molecular anchoring and stabilization. This finding establishes these residues as a key pharmacophore in the design of future *Pf*CDPK-1 inhibitors. The most potent compound, 25172, exhibited the strongest binding affinity (−10.030 kcal/mol), indicating an exceptionally stable and energetically favorable interaction with the target protein. This

high affinity likely arises from a combination of hydrogen bonding with the core residues (Tyr148 and Glu146) and additional, potentially more subtle, interactions with other residues within the binding pocket.In contrast, our docking of the reference compound, purfalcamine, revealed a different binding mode. Purfalcamine formed hydrogen bonds with Arg60, Glu152, Asn196, and Asp212. A significant observation is that while Asn196 and Asp212 are located within the enzyme's active site, Arg60 and Glu152 are found outside the primary binding pocket. This peripheral binding mode, which is distinct from our novel compounds, likely accounts for purfalcamine's lower binding affinity (−8.421 kcal/mol). The recurring involvement of Glu152 in both our lead compounds and purfalcamine's binding further supports its previously established role in ligand stabilization [28,29]. This consistency across different chemical scaffolds strengthens the evidence for its importance in the design of *Pf*CDPK-1 inhibitors.

Compounds against *Pf*CDK-2 revealed a significant improvement in binding affinity compared to the known inhibitor, staurosporine. This provides a strong foundation for identifying more effective anti-malarial agents. Staurosporine exhibited a relatively weak binding affinity (–6.022 kcal/mol), forming a single hydrogen bond with Cys149 and additional hydrophobic and polar contacts. This finding is consistent with its known role as a broad-spectrum kinase inhibitor. The limited number of specific interactions within the *Pf*CDK-2 active site likely contributes to its moderate binding affinity and lack of selectivity. In contrast, our lead compounds—7383, 7384, and 8255—demonstrated significantly stronger binding affinities, ranging from –10.972 to –10.554 kcal/mol. This enhanced stability is attributed to a more robust interaction profile within the enzyme's active site. All three compounds consistently formed crucial hydrogen bonds with Cys149 and Glu147. The shared interaction with these two residues suggests that they are central to the effective anchoring and stabilization of inhibitors, establishing them as a key pharmacophore for a new class of *Pf*CDPK-2 inhibitors. The superior binding of these novel compounds over staurosporine highlights a successful strategy for designing more potent and selective inhibitors. By targeting specific residues (Cys149 and Glu147) that are critical for inhibition, our compounds achieve a more stable binding conformation than the less specific interactions observed with staurosporine. However, against *Pf*CDK-4 revealed that the reference compound Pyrazole 3,4-d Pyrimidine has a relatively weak binding affinity (–5.131 kcal/mol). While it formed hydrogen bonds with Gly74, Tyr150, and Glu154, these interactions were insufficient to achieve a strong overall binding, likely due to a limited number of other stabilizing contacts or an unfavorable binding conformation. In sharp contrast, our lead compounds—17603, 8286, and 6395—exhibited markedly superior binding affinities, ranging from –9.935 to –9.410 kcal/mol. This enhanced stability is attributed to a more robust and specific interaction profile. All three compounds consistently formed crucial hydrogen bonds with Glu154, Tyr150, and Asp148. The conserved nature of these interactions across all three lead compounds suggests that these three residues are not merely involved in binding but are essential for effective molecular anchoring and stabilization. This finding establishes Glu154, Tyr150, and Asp148 as a key pharmacophore for a new class of inhibitors targeting this protein. The superior binding of our novel compounds over the reference highlights a successful strategy for identifying more potent inhibitors by targeting these specific, crucial residues.

Also against *Pf*hexokinase revealed that our novel compounds exhibit superior binding affinities compared to the reference compound, Ebselen. This suggests they are promising candidates for inhibiting this key malaria protein. Ebselen showed a modest binding affinity (–4.003 kcal/mol), forming hydrogen bonds with Ser436 and Thr268. This indicates a relatively weak interaction, likely due to a limited number of stabilizing contacts within the active site. In contrast, our lead compounds 21023 and 21024 achieved significantly stronger binding affinities (–7.423 kcal/mol). This enhanced stability is attributed to their consistent hydrogen bonding with Glu359 and Ser358. The recurring interaction with these two residues suggests they

are critical for effective molecular anchoring and stabilization within the *Pf*Hexokinase active site. Compound 18297 exhibited a unique and robust binding profile, forming multiple hydrogen bonds with a different set of residues, including Thr268, Ser436, and Asn107. This unique binding mode resulted in a strong binding affinity (–7.275 kcal/mol), comparable to the other lead compounds. This suggests the PfHexokinase active site may accommodate diverse chemical scaffolds and binding modes to achieve effective inhibition. These findings highlight that Glu359 and Ser358 are critical residues for ligand stabilization, and our selected compounds represent promising scaffolds for the development of potent PfHexokinase inhibitors.

Our molecular docking analysis against *Pf*LDH revealed that our compounds exhibit significantly stronger binding affinities compared to the reference compound, chloroquine, suggesting their potential as more effective inhibitors. Chloroquine, a well-known anti-malarial, showed a relatively weak binding affinity of –4.673 kcal/mol. Its interactions were limited to hydrogen bonds with Thr97 and Arg171, indicating a modest and likely non-optimal fit within the active site. In sharp contrast, our lead compounds demonstrated markedly superior binding. Compound 12876 exhibited the highest binding affinity at –9.065 kcal/mol. This enhanced stability is attributed to a more extensive network of hydrogen bonds with Arg171, Ile31, and Thr101, with additional interactions with Arg171. The multifaceted interactions of compound 12876 within the binding pocket highlight a more effective binding mode. Compounds 18620 and 18621, which are stereoisomers, also showed strong binding profiles (–8.437 and –8.457 kcal/mol, respectively). Their consistent interactions with His195, Thr97, and Asn140 suggest these residues are crucial for ligand stabilization. The similar binding affinities of these two compounds, despite their stereoisomeric nature, further emphasizes the importance of a conserved interaction pattern for effective binding. These findings collectively underscore the critical role of Arg171, Thr97, and His195 in ligand binding to PfLDH. By targeting these key residues, our novel compounds achieve significantly improved binding affinities over chloroquine, suggesting they may serve as a new class of potent inhibitors with enhanced efficacy against malaria.

The novel *Pf*CDPK-1 inhibitors 25172, 24681, and 25353 showed favorable absorption, with high Human Intestinal Absorption (HIA) (0.91–0.99) and moderate Caco-2 permeability (1.48–2.59). However, their oral bioavailability was suboptimal (18–28%), suggesting significant first-pass metabolism or poor solubility. In contrast, the reference compound purfalcamine had superior bioavailability (55%), but showed significant CYP inhibition, particularly for CYP2C9 and CYP3A4, raising concerns for drug-drug interactions. All compounds had high plasma protein binding (87–92%), which may limit the free drug concentration. A major safety concern was the consistently high genotoxicity scores (0.99–1.00). While all candidates showed some toxicity, compound 24681 had lower hERG inhibition and moderate mutagenicity, suggesting a safer cardiac profile compared to purfalcamine.

The selected *Pf*CDPK-2 inhibitors demonstrated excellent HIA and moderate Caco-2 permeability. Staurosporine, the reference compound, had exceptionally high permeability but a negative clearance value, indicating potential for accumulation. In contrast, compound 8255 had the highest oral bioavailability (42%) and efficient clearance. A positive finding was the minimal P-glycoprotein (P-gp) inhibition (0.05–0.1) for the novel compounds, reducing the risk of efflux-mediated resistance, unlike staurosporine, which showed strong P-gp inhibition. A notable drawback was the high CYP1A2 inhibition (0.93) and elevated CYP induction scores (0.66–0.68) across all candidates, which could lead to drug-drug interactions. The major safety concerns were the high genotoxicity and DILI (drug-induced liver injury) risk. However, the novel compounds showed negligible hERG inhibition and a minimal risk of cardiotoxicity.

The *Pf*CDPK-4 inhibitors displayed strong absorption, with high Caco-2 permeability and HIA. Their oral bioavailability was moderate (30–37%), which is acceptable for oral

formulations. They showed high CYP induction and strong CYP1A2 inhibition, but had low CYP3A4 inhibition, reducing interference with a major metabolic pathway. Toxicity profiles were favorable, with low hERG inhibition, minimal mutagenicity, and moderate hepatic toxicity. While genotoxicity scores were elevated, they were lower than those seen in other inhibitor classes. Compound 8286 had the lowest Hek293 toxicity, suggesting a more favorable overall safety profile.

Compounds 21023 and 21024 showed excellent absorption, with high Caco-2 permeability and HIA for *pf*hexokinase. They had favorable oral bioavailability (56–65%), surpassing the reference compound ebselen (62%). Plasma protein binding was moderate, suggesting more free drug is available. A key advantage was the minimal CYP inhibition for all isoforms (≤0.33), unlike ebselen, which showed strong CYP1A2 inhibition. However, these compounds had low or negative clearance, indicating potential for accumulation. Their toxicity profiles were good with low hERG inhibition, low Ames toxicity, and minimal mutagenicity. Genotoxicity scores were moderate, and hepatic toxicity was lower than ebselen, suggesting an improved safety margin.

The *Pf*LDH inhibitors had moderate absorption, with acceptable Caco-2 permeability and oral bioavailability (38–49%). Although the reference compound chloroquine had higher permeability and bioavailability, it also showed strong P-gp inhibition, which could lead to drug resistance. In contrast, our selected compounds had low P-gp inhibition, which is a desirable characteristic. They also had favorable clearance values and minimal CYP inhibition. Their toxicity profiles were superior to chloroquine, with negligible hERG inhibition, low Hek293 toxicity, and reduced hepatic toxicity. While genotoxicity scores were slightly elevated, mutagenicity remained low, supporting their potential for further investigation.

The MM-GBSA (Molecular Mechanics Generalized Born Surface Area) binding free energy calculations provide a more rigorous thermodynamic assessment of the ligand-protein interactions than simple docking scores. A more negative ΔGBind value indicates a more energetically favorable and stable protein-ligand complex [. The decomposition of this energy into its components—hydrogen bond, van der Waals, and solvation energies—sheds light on the specific forces driving the binding process. Our novel compounds (24681, 25172, and 25353) of *pf*CDK1 demonstrated significantly more favorable total binding free energies compared to the reference compound, purfalcamine. This is largely driven by their highly negative van der Waals energies, which suggest a superior shape complementarity and favorable hydrophobic packing within the enzyme's active site. The more negative hydrogen bond energies of our compounds also underscore their ability to form stronger hydrogen bonds, which further contributes to enhanced binding stability [30,31]. The novel *Pf*CDPK2 inhibitors (7483, 7484, and 8255) exhibited markedly improved binding free energies over staurosporine. The primary force behind this is the significantly more negative hydrogen bond energies and van der Waals interactions. The highly favorable van der Waals energy of compound 7483 suggests a particularly good fit within the active site. While the solvation energies for these compounds are less favorable, the strong interaction energies in the bound state are sufficient to overcome the energetic cost of desolvation [32]. Compounds 6395, 8286, and 17603 of PfCDPK4 showed a substantial improvement in binding free energies compared to pyrazole-3,4-d pyrimidine. This is attributed to their more negative hydrogen bond and van der Waals energies. Notably, compounds 8286 and 17603 also had highly favorable solvation energies, indicating that their binding process is energetically favorable in terms of solvent release [33]. The selected LDH inhibitors (12876, 18620, and 18621) had a much more negative binding free energy than chloroquine. This superior binding is driven by significantly more favorable hydrogen bond and van der Waals energies. While their solvation energies were less favorable than chloroquine’s, the strong interactions in the bound state more than compensate for this. Compound 12876 stands out with the most negative overall binding energy [34]. The hexokinase inhibitors (18297, 21023, and 21024) demonstrated a remarkable improvement in

binding free energies over ebselen. This is overwhelmingly driven by more favorable hydrogen bond and van der Waals energies. Although their solvation energies are less favorable, this is a common trade-off where strong interactions in the binding pocket outweigh the energy cost of desolvation. Compound 21023 had the most negative overall binding energy, indicating the highest predicted binding stability [35]. Computer-Aided Drug Design (CADD) utilizes various in silico tools and techniques to optimize and accelerate multiple stages of the drug discovery process, which is critical for reducing the overall research and development time and cost [36, 37]. It is a predictive model that needs to be validated either through *in vivo* and *in vitro* studies.

Conclusion

In this study *in silico* approach was used to identify and characterize novel inhibitors for five crucial proteins in *Plasmodium falciparum*: *Pf*CDPK-1, *Pf*CDPK-2, *Pf*CDPK-4, *Pf*Hexokinase, and *Pf*LDH. Our molecular docking and subsequent MM-GBSA calculations consistently demonstrated that several novel compounds possess significantly more favorable binding affinities than their respective reference compounds. The structural analog analysis provided critical insights into the structure-activity relationships (SARs). We successfully identified key pharmacophore motifs—such as the indole ring system—and pinpointed specific amino acid residues (Tyr148, Glu146, Cys149, Glu147, and Arg171) that are essential for strong ligand binding and stabilization. This detailed understanding of the molecular interactions provides a clear roadmap for designing more potent and selective next-generation inhibitors. The ADMET evaluation revealed a mixed but ultimately promising profile for our top candidates. While some compounds faced challenges like suboptimal oral bioavailability and high genotoxicity scores, others exhibited favorable absorption, efficient metabolism, and low-risk profiles for critical off-target effects like hERG inhibition. For instance, the Hexokinase inhibitors showed excellent absorption and low toxicity, while some CDPK-4 inhibitors displayed a favorable balance of efficacy and safety.

In summary, this study identifies a series of potent new compounds against malaria targets and provides a robust computational framework for their continued development. The most promising compounds, particularly those with a strong binding profile and a favorable ADMET risk assessment, are lead compounds for further experimental validation. However, a major limitation of the current findings is that absence of data on molecular dynamics (MD) simulations to model the flexibility and stability of the protein-ligand complexes over specific period. Additionally, studies involving protein target inhibition and *in vitro* antimalarial assessment are required to validate the computational findings. We recommend that future work focuses on the synthesis and *in vitro* testing of these candidates to confirm their anti-malarial activity, followed by lead optimization to address identified liabilities and develop them into safe and effective therapeutic agents.

Declarations

Acknowledgments

Department of Biochemistry, Bowen University, Iwo, Nigeria.

Conflict of interest

The authors declare no conflict of interest.

Data Availability Statement

All data used are as presented in the review article.

Funding Statement

The study received no external funding.

Ethics approval

Not applicable

Informed consent

Not applicable

Author Contribution

MPO, GB & OSA conceived the study; MPO and TOO acquired the data and performed the data analysis; MPO and TOO wrote the original manuscript; GB & OSA supervised the work; GB & OSA reviewed the original manuscript. All authors read and approved the final manuscript.

References

[1] Al-Worafi, Y. M. (2024). Malaria management in developing countries. In *Handbook of Medical and Health Sciences in Developing Countries: Education, Practice, and Research* (pp. 1-40). Cham: Springer International Publishing.

[2] Johnson, I. U., Asuquo, A. E., & Izah, S. C. (2024). Epidemiological Trends and Public Health Strategies in Malaria Control: A Global Perspective. *ES General*, *7*, 1365.

[3] Manzoni, G., Try, R., Guintran, J. O., Christiansen-Jucht, C., Jacoby, E., Sovannaroth, S., ... & Tuseo, L. (2024). Progress towards malaria elimination in the Greater Mekong Subregion: perspectives fro m the World Health Organization. *Malaria journal*, *23*(1), 64.

[4] Jezewski, A. J., Lin, Y. H., Reisz, J. A., Culp-Hill, R., Barekatain, Y., Yan, V. C., ... & Odom John, A. R. (2021). Targeting host glycolysis as a strategy for antimalarial development. *Frontiers in Cellular and Infection Microbiology*, *11*, 730413.

[5] Belete, T. M. (2020). Recent progress in the development of new antimalarial drugs with novel targets. *Drug design, development and therapy*, 3875-3889.

[6] Shibeshi, M. A., Kifle, Z. D., & Atnafie, S. A. (2020). Antimalarial drug resistance and novel targets for antimalarial drug discovery. *Infection and drug resistance*, 4047-4060.

[7] Ong, H. W., Adderley, J., Tobin, A. B., Drewry, D. H., & Doerig, C. (2023). Parasite and host kinases as targets for antimalarials. *Expert Opinion on Therapeutic Targets*, *27*(2), 151-169.

[8] Makungo, T. (2016). *The search for novel compunds targeting PfCDPK4 for therapeutic treatment of Malaria* (Doctoral dissertation).

[9] Niniola, O. (2025). *Characterising Plasmodium falciparum cyclin dependent like kinase 1 (PfCLK1) as a potential antimalarial target* (Doctoral dissertation, University of Glasgow).

[10] Soni, R., Sharma, D., Rai, P., Sharma, B., & Bhatt, T. K. (2017). Signaling strategies of malaria parasite for its survival, proliferation, and infection during erythrocytic stage. *Frontiers in immunology*, *8*, 349.

[11] Dillenberger, M., Werner, A. D., Velten, A. S., Rahlfs, S., Becker, K., & Fritz-Wolf, K. (2023). Structural analysis of Plasmodium falciparum hexokinase provides novel information about catalysis due to a Plasmodium-specific insertion. International Journal of Molecular Sciences, 24(16), 12739.

[12] Jortzik, E., & Becker, K. (2011). Energy Metabolism as an Antimalarial Drug Target. *Apicomplexan Parasites: Molecular Approaches toward Targeted Drug Development*, 75-95.

[13] Naidoo, K. (2012). *The role of glycerol kinase in Plasmodium falciparum*. University of the Witwatersrand, Johannesburg (South Africa).

[14] Butler, J. H. (2021). *Antimalarial Drug Discovery from Natural Products* (Doctoral dissertation, University of Georgia).

[15] Pérez-Victoria, I. (2024). Natural Products Dereplication: Databases and Analytical Methods. *Progress in the Chemistry of Organic Natural Products 124*, 1-56.

[16] Rutz, A., Sorokina, M., Galgonek, J., Mietchen, D., Willighagen, E., Gaudry, A., ... & Allard, P. M. (2022). The LOTUS initiative for open knowledge management in natural products research. *elife*, *11*, e70780.

[17] Fokou, P. V. T., Tali, M. B. T., Mbouna, C. D. J., Yamthe, L. R. T., Sharifi-Rad, J., Calina, D., ... & Boyom, F. F. (2025). Natural products as transmission-blocking agents against malaria: a comprehensive review of bioactive compounds and their therapeutic potential. *Malaria Journal*, *24*(1), 164.

[18] Van Santen, J. A., Poynton, E. F., Iskakova, D., McMann, E., Alsup, T. A., Clark, T. N., ... & Linington, R. G. (2022). The Natural Products Atlas 2.0: a database of microbially-derived natural products. *Nucleic acids research*, *50*(D1), D1317-D1323.

[19] Armstrong, J. F., Campo, B., Alexander, S. P., Arendse, L. B., Cheng, X., Davenport, A. P., ... & Davies, J. A. (2023). Advances in malaria pharmacology and the online guide to MALARIA PHARMACOLOGY: IUPHAR review 38. *British Journal of Pharmacology*, *180*(15), 1899-1929.

[20] Tess, D., Chang, G. C., Keefer, C., Carlo, A., Jones, R., & Di, L. (2023). In vitro-in vivo extrapolation and scaling factors for clearance of human and preclinical species with liver microsomes and hepatocytes. *The AAPS Journal*, *25*(3), 40.

[21] Lipinski, C.A., et al. (2001). Experimental and computational approaches to estimate solubility and permeability in drug discovery and development settings. *Adv. Drug Deliv. Rev.*, 46(1–3), 3–26.

[22] Shao, Y., Hong, L., Xie, T., Zhou, B., Wu, J., Cheng, M., ... & Chen, L. (2019, August). iDrug: Pediatric Drug Interaction Modeling and Risk Evaluation Leveraging Prescription Big Data. In 2019 IEEE SmartWorld, Ubiquitous Intelligence & Computing, Advanced & Trusted Computing, Scalable Computing & Communications, Cloud & Big Data Computing, Internet of People and Smart City Innovation (SmartWorld/SCALCOM/UIC/ATC/CBDCom/IOP/SCI) (pp. 700-706). IEEE.

[23] Zhang, V., Chavchich, M., & C. Waters, N. (2012). Targeting protein kinases in the malaria parasite: update of an antimalarial drug target. *Current topics in medicinal chemistry*, *12*(5), 456-472.

[24] Giménez, B. G., Santos, M. S., Ferrarini, M., & Fernandes, J. P. S. (2010). Evaluation of blockbuster drugs under the rule-of-five. *Die Pharmazie-An International Journal of Pharmaceutical Sciences*, *65*(2), 148-152.

[25] Alam, A., Neyaz, M. K., & Ikramul Hasan, S. (2014). Exploiting unique structural and functional properties of malarial glycolytic enzymes for antimalarial drug development. *Malaria Research and Treatment*, *2014*(1), 451065

[26] Luthman, K., & Steffansen, B. (2010). Chemical approaches to improving bioavailability properties of oral drug candidates. *Molecular Biopharmaceutics*, 71.

[27] Shukla, S., Kushwah, S., & Mani, A. (2025). Targeting Malaria's Achilles' Heels: A Review of Plasmodium Life Cycle Vulnerabilities for Drug Discovery. *Current Topics in Medicinal Chemistry*.

[28] Chang, S., Zhang, L., Xu, S., Luo, J., Lu, X., Zhang, Z., ... & Ding, K. (2012). Design, synthesis, and biological evaluation of novel conformationally constrained inhibitors targeting epidermal growth factor receptor threonine790→methionine790 mutant. *Journal of Medicinal Chemistry*, *55*(6), 2711-2723.

[29] Ong, H. W., Adderley, J., Tobin, A. B., Drewry, D. H., & Doerig, C. (2023). Parasite and host kinases as targets for

antimalarials. *Expert Opinion on Therapeutic Targets*, *27*(2), 151-169.

[30] Dosoky, N. S., Shah, S. A., Dawson, J. T., Banjara, S. S., Poudel, A., Bascoul, C., & Satyal, P. (2023). Chemical composition, market survey, and safety assessment of blue lotus (Nymphaea caerulea Savigny) extracts. *Molecules*, *28*(20), 7014.

[31] Cheuka, P. M., Njaria, P., Mayoka, G., & Funjika, E. (2024). Emerging drug targets for antimalarial drug discovery: validation and insights into molecular mechanisms of function. *Journal of Medicinal Chemistry*, *67*(2), 838-863

[32] Kugelstadt, D., Derrer, B., & Kappes, B. (2011). Calcium-Dependent Protein Kinases as Drug Targets in Apicomplexan Parasites. *Apicomplexan Parasites: Molecular Approaches toward Targeted Drug Development*, 319-333.

[33] Utami, P. D., Yudo, V., & Budiarti, R. (2024). Blockade of Multiple Pathways of P. falciparum by Quinoxaline from Curry Fish (S. hermanni) Using an in silico Approach. *Indian Journal of Pharmaceutical Education and Research*, *59*(1), 326-337.

[34] .Maharao, N., Antontsev, V., Wright, M., & Varshney, J. (2020). Entering the era of computationally driven drug development. *Drug Metabolism Reviews*, *52*(2), 283-298.

[35] 34.Armstrong, J. F., Campo, B., Alexander, S. P., Arendse, L. B., Cheng, X., Davenport, A. P., ... & Davies, J. A. (2023). Advances in malaria pharmacology and the online guide to MALARIA PHARMACOLOGY: IUPHAR review 38. *British Journal of Pharmacology*, *180*(15), 1899-1929.

[36] 35.Noori, Ortega, S. S., Cara, L. C. L., & Salvador, M. K. (2012). In silico pharmacology for a multidisciplinary drug discovery process. *Drug metabolism and drug interactions*, *27*(4), 199-207.

[37] 36. Cheng F, Li W, Liu G, Tang Y. In silico ADMET prediction: recent advances, current challenges and future trends. Curr Top Med Chem. 2013;13(11):1273–1289. doi: 10.2174/15680266113139990033.

[38] 37. Daina A, Blatter MC, Baillie Gerritsen V, Palagi PM, Marek D, Xenarios I, et al. Drug design workshop: A web based educational tools to introduce Computer Aided Drug Design to the general public. Journal of chemical education. 2017;94 (3):335-44.